Supporting Information

Glycosylated and rhodamine-conjugated tetraphenylethylene: a type I and II reactive oxygen species generator for photodynamic therapy

Jia-wei Zhang[a], Gai-li Feng[a], Xin Niu[a], Yi-chen Liu[a], Wei Zhou[a], Qing-yu Ma[a], Guang-jian Liu[a], Yuan Zhang*[ab] and Guo-wen Xing*[a]

[a.] *College of Chemistry, Beijing Normal University, Beijing, 100875, China.*

E-mail: yuanzhang@bnu.edu.cn, gwxing@bnu.edu.cn

[b.] *Key Laboratory of Energy Conversion and Storage Materials, College of Chemistry, Beijing Normal University, Beijing, 100875, China*

Experimental Section

Materials and instruments

Unless otherwise stated, chemicals and solvents were of reagent grade and used as obtained from commercial sources without further purification. HepG2 cells were obtained from Beijing Keling Biochemical Technology Research Institute. The commercial dyes for living cells labeling were purchased from Beyotime. All reactions are carried out under magnetic stirring. Reactions are monitored by the analytical thin layer chromatography (TLC) on the silica F254 glass plate and displayed by UV light (254nm or 365nm) or immersed in EtOH-H_2SO_4 (4%) before heating. Nuclear magnetic resonance (^{1}H and ^{13}C NMR) spectra were measured at room temperature with JEOL's NMR (400 or 600 MHz) spectrometer. Mass spectra were recorded on a waters LCT Premier XEmass spectrometer. Transmission electron microscope (TEM) images were recorded on FEI Talos F200S. Dynamic Light Scattering (DLS) measurements were performed on a Zeta potential analyzer (Brookhaven Instruments Corporation, America). Fluorescence spectra were measured on FS5 and UV-Vis spectra were recorded on Shimadzu UV-3600. Confocal fluorescence imaging was performed with Nikon A1R MP multiphoton microscopy. Irradiation was performed using a LED light (PLS-LED 100, Perfect Light, Beijing, China). All optical testing experiments were performed in PBS solution (10 mM, pH 7.4).

Total Reactive oxygen species (ROS) detection in solution

Configure 3 mL of test solution containing 25 μM DCFH and 10 μM photosensitizer in PBS or DMSO. After irradiated by LED irradiation (400-800 nm, 40 mW cm^{-2}), the fluorescence signal of DCFH was monitored to indicate the ROS generation with the excitation wavelength of 488 nm and the emission wavelength of 522 nm.

Singlet oxygen ($^1O_2$) detection in solution

Configure 3 mL of test solution containing 10 μM ABDA and 10 μM photosensitizer in PBS. After irradiated by LED irradiation (400-800 nm, 40 mW cm^{-2}), the absorption signal of the indicator was monitored, and the decrease in the absorption signal at 379 nm indicated the $^1O_2$ generation.

Detection of type I ROS production with DHR123 and Vc in solution

Dihydrorhodamine 123 (DHR123) was used as an indicator for detection of type I ROS and Vitamin C (Vc) was as a scavenger for radical. Configure 3 mL of test solution containing 15 μM DHR123 and 10μM photosensitizer in PBS and the experimental group with Vc is additionally added with 100 μM Vc. After irradiated by LED irradiation (400-800 nm, 40 mW cm^{-2}), the fluorescence signal of

DHR123 was monitored to indicate the $O_2^{-\bullet}$ generation with the excitation wavelength of 488 nm and the emission wavelength of 527 nm.

Confocal imaging of living cells

HepG2 and HeLa cells were cultured in Dulbecco's modified Eagle's medium (DMEM) supplemented with 10% FBS, penicillin (100 μg/mL), and streptomycin (100 μg/mL) at 37 °C in a humidified incubator, and culture media were replaced with fresh media every day. The cells were further incubated with diverse concentration of probes in culture media at 37 °C and then washed it with PBS for three times to remove the dye in the solution before cell fluorescence imaging experiments with confocal laser scanning microscopy. For cells treated with Lac-TRs, the red fluorescence intensity in the cells was observed with the Nikon single-particle microscope: λ_{ex} = 561 nm, λ_{em} = 580-700 nm.

Intracellular ROS detection

2,7-Dichlorodihydrofluorescein diacetate (DCFH-DA) was as the fluorescent indicator for total ROS. Briefly, HepG2 cells were incubated with 10 μM Lac-TRs for 3 h under normoxic (21% O_2) or hypoxic (2% O_2) conditions and then washed with PBS three times. Then, the cells were incubated with the fluorescent probe DCFH-DA (15 μM) for 30 min at 37°C in the dark, and then were washed three times with PBS. Cells were subsequently treated with LED irradiation (400-800 nm, 40 mW cm^{-2}) for 10 min or in the dark and then serially examined with the Nikon single-particle microscope with a 40 × objective lens. The green fluorescence intensity of the indicators in the cells was observed: λ_{ex} = 488 nm, λ_{em} = 500-550 nm.

Intracellular type I ROS production

Dihydrorhodamine 123 (DHR123,10 μM) was as the fluorescent indicator for type I ROS production and Vitamin C (Vc) was as a scavenger for radical. HepG2 cells were incubated with 10 μM Lac-TRs for 3 h and for the Vc-added group, cells were incubated with Vc (100 μM) for 1 h before adding Lac-TRs for incubation, and the subsequent steps were the same. After light irradiation (40 mW cm^{-2}, 400-800 nm) for 10 min or in the dark and then serially examined with the Nikon single-particle microscope with a 40 × objective lens. The green fluorescence intensity of the indicators in the cells was observed: λ_{ex} = 488 nm, λ_{em} = 500-550 nm.

Intracellular $O_2^{-\bullet}$ detection

Dihydroethidium (DHE) was as the fluorescent indicator for $O_2^{-\bullet}$. Briefly, HepG2 cells were incubated with 10 μM Lac-TRs for 3 h under normoxic (21% O_2) or hypoxic (2% O_2) conditions and then washed

with PBS three times. Then, the cells were incubated with the fluorescent probe DHE (5 μM) for 30 min at 37°C in the dark, and then were washed three times with PBS. Irradiated group cells were subsequently treated with LED irradiation (400-800 nm, 40 mW cm^{-2}) for 10 min and then serially examined with the Nikon single-particle microscope with a 40 × objective lens. The red fluorescence intensity of the indicators in the cells was observed: λ_{ex} = 488 nm, λ_{em} = 580-620 nm.

Co-localization imaging

HepG2 cells were first stained using Lac-TRs at a concentration of 10 μM for 3 h. After washing with PBS, cells were incubated with 1μM each of Mito Tracker Green and Lyso Tracker Green for 30 min and washed three times with PBS before taking confocal images. After fluorescence images were collected, the analysis was performed with Image J. software. The green fluorescence intensity of the indicators in the cells was observed: λ_{ex} = 488 nm, λ_{em} = 500-550 nm.

Live/dead cell staining

The HepG2 and Hela cells were incubated with Lac-TRs (10 μM) for 3 h. And washing off the residual dye, the cells were irradiated with a LED light (400–800 nm, 40 mW cm^{-2}) for 10 min or in the dark, after the treatment, the cells were further cultured for 30 min. Finally, the cells were stained with Calcein-AM/PI mixtures (5 μM for Calcein-AM, 5 μM for PI) for 30 min. Fluorescent images were promptly captured by Nikon single-particle microscopy with 10 × objective lens. The green fluorescence intensity of the Calcein-AM in the cells was observed: λ_{ex} = 488 nm, λ_{em} = 500-550 nm. The red fluorescence intensity of the PI in the cells was observed: λ_{ex} = 488 nm, λ_{em} = 580-620 nm.

$O_2^{-\bullet}$ and $^1O_2$ detection by ESR spectroscopy.

5,5-dimethyl-1-pyrroline-N-oxide (DMPO) and 2,2,6,6-tet-ramethyl-4-piperidone (TEMP) was applied as the spintrap agent for $O_2^{-\bullet}$ and $^1O_2$, respectively. Briefly, Lac-TR was prepared as 50 μM solutions in water and TEMP or DMPO (20mM) was added to the solution. Then, each cuvette was illuminated with a xenon lamp (500–1200 nm). The EPR signal were measured immediately after photoirradiation.

Cyclic Voltammetry Measurement.

Cyclic voltammetry experiments were conducted using a three-electrode system. The platinum- carbon composite electrode was used as the working electrode, while the Pt wire electrode and Ag/AgCl electrode serve as the auxiliary electrode and reference electrode, respectively. The measurement was containing 0.1 M tetrabutylammonium hexafluorophosphate as the supporting electrolyte. The scan

rate was optimized as 100 mV s^{-1}. Fc/Fc+ was used as an external reference.

The measurement of photocurrent responses.

The photocurrent responses experiment was carried out using a three-electrode configuration. A platinum-carbon compound electrode was used as working electrode, the Pt wire electrode and the Ag/AgCl electrode were used as the auxiliary electrode and reference electrode, respectively. The measurement was conducted containing 0.1 M KCl as the supporting electrolyte. The system was irradiated with a xenon lamp (400-800 nm) at an intensity of 80 mW cm^{-2}, and measurements were taken at 30-second intervals.

Computational details.

The optimization of Lac-TR was carried out by DFT calculation at b3lyp/6-31G(d) level with Grimme's dispersion with D3 damping function. The calculation of excited state energies was carried out by time-dependent DFT (TD-DFT) at the same computation level. All the DFT calculations were performed using Gaussian09 (Revision D.01) package[1,2,3,4]. The HOMO-LUMO energy gap and intramolecular interaction forces was analyzed using Multiwfn 3.8 software[5].

Cell ablation study (MTT assay)

The viabilities of cells were evaluated by methylthiazolyldiphenyltetrazolium bromide (MTT) assays. Briefly, the cells were seeded onto 96-well plates and cultured for 24 h. Then, the cells were incubated with various concentration of Lac-TRs for 3 h, followed by replacing the Lac-TR solution with fresh DMEM. The cells were washed and illuminated by LED light source (400-800 nm, 40 mW cm^{-2}) for 10 min or in the dark, the cells were further cultured for 15 h. 10 μL MTT solution (5 mg mL^{-1}) was added into each well, and further cultured for 4 h. After removing liquid supernatant, 100 μL DMSO was added into each well to dissolve the crystals. The absorption of each well at 490 nm was recorded via a plate reader. For the hypoxia experimental group, the operation was carried out in the Hypoxia Incubator Chamber, and the rest of the operations were the same. For the dark toxicity test, the light process is omitted, and the rest of the operations are consistent with the phototoxicity test.

Flow Cytometry Test of pyroptosis

HepG2 cells were seeded onto 6-well plates and cultured for 24 h. Then the cells were incubated with 15 μM or 20 μM Lac-TRs and washed with fresh DMEM. Then, the cells were irradiated with a LED light (400-800 nm, 40 mW cm^{-2}). After further incubation for 0.5 h, the cells were collected and treated with AnnexinV-FITC/PI cell death detection kit. The flow cytometry was used to detect cell death.

LDH release assays

Briefly, HepG2 cells were seeded onto 96-well plates and cultured for 24 h. Then the cells were

incubated with 10 μM **Lac-TR** for 3 h and washed with fresh DMEM. The light groups were irradiated with LED light source (400-800 nm, 40 mW cm^{-2}) and the release of lactate dehydrogenase (LDH) into the cell supernatants was detected using an LDH kit (LDH Release Assay Kit was purchased from Beyotime, catalogue # C0016) according to the manufacturer's instructions.

Western Blot

After treatment with the studied compound, cells were harvested and washed with cold PBS. After incubating in cell lysis buffer for Western and IP (Beyotime, catalogue # P0013), the cell lysates were sonicated and centrifuged (4℃, 12000 rpm 15 min). The protein concentration was determined using a BCA (bicinchoninic acid) kit. The proteins from SDS polyacrylamide gel were separated by electrophoresis and transferred to a polyvinylidene fluoride (PVDF) membrane. PVDF membrane was continued to be enclosed in 5% skim milk powder for 1 h, and then incubated with primary antibody GSDMD-N (Abcam, catalogue # ab215203) and β-actin (Affinity, catalogue # AF7018) at 4℃ overnight. The secondary antibody was incubated for 2 h at room temperature, and the results were obtained by exposure.

Synthesis of Lac-TR

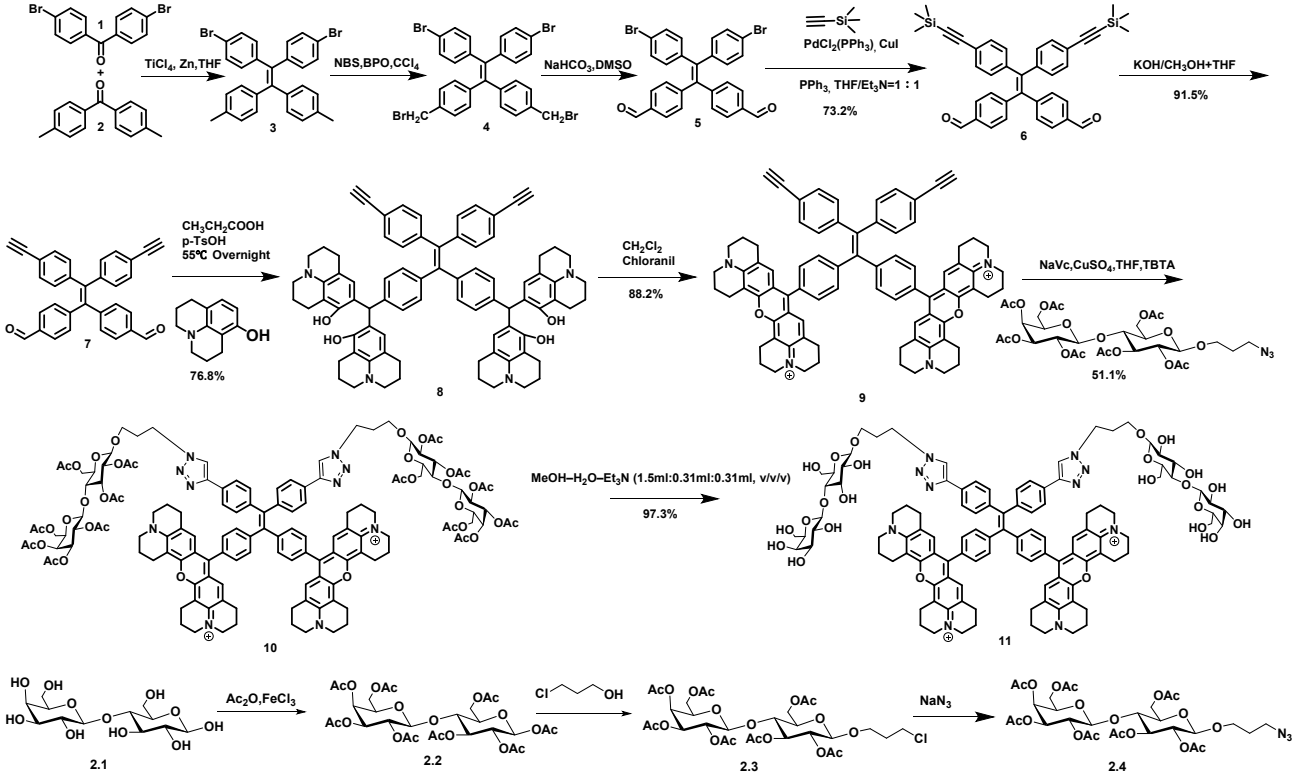

Scheme S1. Synthetic route for Lac-TR

Compounds **3**-**5**[6] and **2.1**-**2.4**[7, 8] were synthesized according to the procedures in the literatures.

Synthesis of Compound 6: Under nitrogen protection, into a 50 mL high-pressure reaction tubes $PdCl_2(PPh_3)_2$ (0.0154g, 0.0220 mmol), CuI (0.00837g, 0.0439 mmol), PPh_3 (0.0173g, 0.0659 mmol), Compound **5** (0.200 g, 0.366mmol), and finally a mixture of THF and triethylamine (TEA) (1:1 v/v) (6 mL) were added under nitrogen. After homogenization of the mixture, trimethylsilylacetylene (0.129 mL, 0.915 mmol) was injected. The solution was hold at 70 °C for 10 h, after which the formed solid was removed by filtration and washed with water. The filtrate was concentrated by a rotary evaporator, and the crude product was purified by silica gel column chromatography using petroleum ether /ethyl acetate mixture (v/v 100:2) as eluent. A yellow solid was obtained (0.156 g, 73.2%). ^{1}HNMR (400 MHz, Chloroform-d) δ 10.02 (s, 2H), 7.75 (d, J = 7.0 Hz, 4H), 7.33 (d, J = 7.1 Hz, 4H), 7.25 (d, J = 7.2 Hz, 4H), 7.02 (d, J = 7.3 Hz, 4H), 0.32 (s, 18H). ^{13}C NMR (100 MHz, Chloroform-d) δ 191.95, 149.27, 143.83, 142.61, 140.06, 135.24, 132.23, 132.09, 131.53, 129.88, 122.72, 104.96, 95.87, 0.28.

Synthesis of Compound 7: Compound **6** (0.150g,0.258mmol) was placed in a 25 mL single-mouth bottle and dissolved by adding tetrahydrofuran (3 mL). The potassium hydroxide solid (0.0579 g, 1.034

mmol) was weighed and dissolved in methanol (1.3 mL) to obtain a solution, and the solution was added dropwise to the reaction system of a single-mouth bottle. The reaction was stirred at room temperature for 3.5 h. After the reaction was monitored, the reaction was quenched to neutral with 1M HCl. Then, the reaction solution was extracted with methylene chloride and washed with saturated salt water. The following process was to dry organic phase with anhydrous magnesium sulfate and remove the solvent by a rotary evaporator. Finally, the obtained solid was purified by column chromatography with petroleum ether /ethyl acetate mixture (v/v 100:3) A yellow solid was obtained. Yield: 0.103 g (91.5 %).^{1}H NMR (400 MHz, Chloroform-d) δ 9.89 (s, 2H), 7.63 (d, J = 8.0 Hz, 4H), 7.23 (d, J = 8.3 Hz, 4H), 7.14 (d, J = 8.1 Hz, 4H), 6.94 (d, J = 8.2 Hz, 4H), 3.06 (s, 2H). ^{13}C NMR (100 MHz, Chloroform-d) δ 191.64, 148.80, 143.22, 142.56, 140.02, 134.95, 131.94, 131.88, 131.24, 129.57, 121.43, 83.26, 78.38.

Synthesis of Compound 8：Under nitrogen protection, compound **7** (0.100 g, 0.229 mmol), 8-Hydroxyjulolidine (0.195 g, 1.0305 mmol), and catalytic amount of *p*-toluenesulfonic acid (0.004 g, 0.0232 mmol) were placed in a 25 mL double necked bottle. Then inject propionic acid, stirred and heated to 50 ℃ for 10 hours. After the reaction is complete, to use an oil pump to spin dry and the obtained solid dissolve in dichloromethane, and rinsed with saturated sodium bicarbonate, saturated saline solution, and water. The following process was to dry organic phase with anhydrous magnesium sulfate and remove the solvent by a rotary evaporator. Finally, the obtained solid was purified by column chromatography with petroleum ether /ethyl acetate mixture (v/v 10:1). A green solid was obtained, Yield: 0.204 g (76.8 %).^{1}H NMR (400 MHz, Chloroform-d) δ 7.23 (d, J = 8.3 Hz, 5H), 6.98 (s, 2H), 6.96 (s, 2H), 6.96 – 6.93 (m, 7H), 6.23 (s, 4H), 5.26 (s, 1H), 4.96 (s, 3H), 3.07 (s, 16H), 3.03 (s, 2H), 2.61 (s, 16H), 2.04 (s, 2H), 1.95 (s, 16H). ^{13}C NMR (150 MHz, Chloroform-d) δ 150.39, 144.09, 143.20, 142.85, 141.18, 140.80, 139.18, 131.49, 131.38, 131.27, 128.81, 127.02, 120.07, 115.17, 114.14, 109.23, 83.76, 77.27, 60.36, 50.08, 49.45, 46.55, 29.65, 27.19, 22.38, 21.67, 21.17. HRMS (ESI): m/z calcd for $[C_{80}H_{76}N_4O_4+2H]^{2+}$: 579.3006; Found: 579.3010

Synthesis of Compound 9：Compound **8** (0.110 g, 0.0951 mmol) were placed in a 25.0 mL single mouthed bottle, dissolved in 3.00 mL of methanol and 3.00 mL of dichloromethane. Then added tetrachlorobenzoquinone (0.0688g,0.28mmol) and stirred at room temperature for about 2.5 hours. The following process was removed the solvent by a rotary evaporator. Finally, the obtained solid was purified by column chromatography with CH_2Cl_2/MeOH (20/1, v/v). A purple solid was obtained. Yield: 0.0939g (88.2%). ^{1}H NMR (400 MHz, Chloroform-d) δ 7.33 (d, J = 7.5 Hz, 4H), 7.27 (d, J = 7.9 Hz, 4H), 7.13 (d, J = 7.5 Hz, 4H), 7.03 (d, J = 7.8 Hz, 4H), 6.70 (s, 4H), 3.50 (s, 16H), 3.09 (s,

2H), 2.96 (s, 8H), 2.73 (s, 8H), 2.00 (d, J = 32.2 Hz, 16H). ^{13}C NMR (100 MHz, Chloroform-d) δ 154.05, 152.22, 151.18, 143.81, 143.29, 142.63, 141.12, 131.78, 131.61, 131.52, 129.63, 126.69, 123.86, 121.08, 112.61, 105.39, 83.41, 78.37, 53.58, 51.11, 50.56, 29.73, 27.90, 20.77, 19.98, 19.79. MS (ESI): m/z calcd for $[C_{80}H_{70}N_4O_2]^{2+}$: 559.27; Found: 559.28

Synthesis of Compound 10：9 (0.0500 g, 0.0447 mmol) and **2-4** (0.0643 g, 0.0894 mmol) were dissolved in 3 mL tetrahydrofuran to obtain a reaction system solution. TBTA (0.0189 g, 0.0358 mmol) was mixed with 1 mL of $CuSO_4$ solution dissolved in water (0.009 g, 0.0358 mmol), dispersed by ultrasound, then add 1 mL of sodium ascorbate solution dissolved in water (0.0142 g, 0.0715 mmol). Add the mixture to the reaction system solution, assisted by ultrasound, and react at room temperature under nitrogen atmosphere for 20 hours. Then, the reaction solution was extracted with methylene chloride and washed with water. The following process was to dry organic phase with anhydrous magnesium sulfate and remove the solvent by a rotary evaporator. Finally, the obtained solid was purified by column chromatography with CH_2Cl_2/MeOH (v/v 10:1). A purple solid was obtained. Yield: 0.0584 g (51.1 %).^{1}H NMR (400 MHz, Chloroform-d) δ 7.67 (s, 2H), 7.37 (s, 3H), 7.13 (s, 13H), 6.72 (s, 4H), 5.25 (d, J = 18.5 Hz, 3H), 5.02 (s, 2H), 4.90 (s, 5H), 4.43 (s, 7H), 4.03 (s, 7H), 3.83 (s, 5H), 3.46 (s, 23H), 2.94 (s, 8H), 2.65 (s, 8H), 2.00 (s, 48H), 1.89 (s, 14H). ^{13}C NMR (150MHz, Chloroform-d) δ 170.41, 170.17, 170.09, 169.78, 169.16, 154.49, 152.24, 151.18, 132.06, 131.70, 129.50, 126.85, 125.31, 123.99, 112.69, 105.19, 101.24, 101.02, 100.66, 76.18, 72.78, 71.72, 71.01, 70.70, 69.17, 66.68, 61.91, 60.81, 51.13, 50.48, 47.02, 31.93, 31.65, 29.70, 29.37, 27.86, 22.70, 20.88, 20.67, 20.53, 19.97, 19.82. MS (ESI): m/z calcd for $[C_{138}H_{152}N_{10}O_{38}]^{2+}$: 1278.51; Found: 1278.50

Synthesis of Compound 11: 10 (0.05 g, 0.0195 mmol) was suspended in distilled MeOH–water–triethylamine (1.5 mL : 0.31 mL : 0.31 mL, v/v/v). The mixture was stirred under nitrogen at room temperature for 2 days. Solvents were evaporated, co-evaporated with toluene three times, and the solid was dissolved in pure water (5 mL) and freeze-dried to get purple flocculent object. Yield: 0.0373g (97.3%). ^{1}H NMR (400 MHz, DMSO-d6) δ 8.57 (s, 2H), 7.75 (s, 4H), 7.41 (s, 4H), 7.18 (s, 8H), 6.63 (s, 4H), 5.24 (s, 2H), 5.05 (s, 5H), 4.78 (s, 5H), 4.67 (s, 7H), 4.53 (s, 22H), 4.15 (s, 13H), 2.94 (s, 16H), 2.53 (s, 7H), 2.09 (s, 9H), 1.76 (s, 16H). ^{13}C NMR (150 MHz, DMSO-D6) δ 153.77, 151.89, 151.11, 146.34, 144.34, 142.60, 132.12, 131.54, 130.17, 129.80, 129.23, 126.30, 125.21, 124.06, 122.37, 112.28, 105.50, 104.45, 103.05, 99.01, 81.43, 79.73, 79.52, 79.30, 76.06, 75.47, 75.38, 73.83, 73.68, 72.18, 71.36, 71.13, 68.59, 65.92, 61.04, 60.88, 55.42, 53.13, 50.82, 50.30, 47.17, 30.52, 30.36, 29.52, 27.68, 20.61, 19.86, 19.67. HRMS (ESI): m/z calcd for $[C_{110}H_{124}N_{10}O_{24}]^{2+}$: 984.4389; Found: 984.4395.

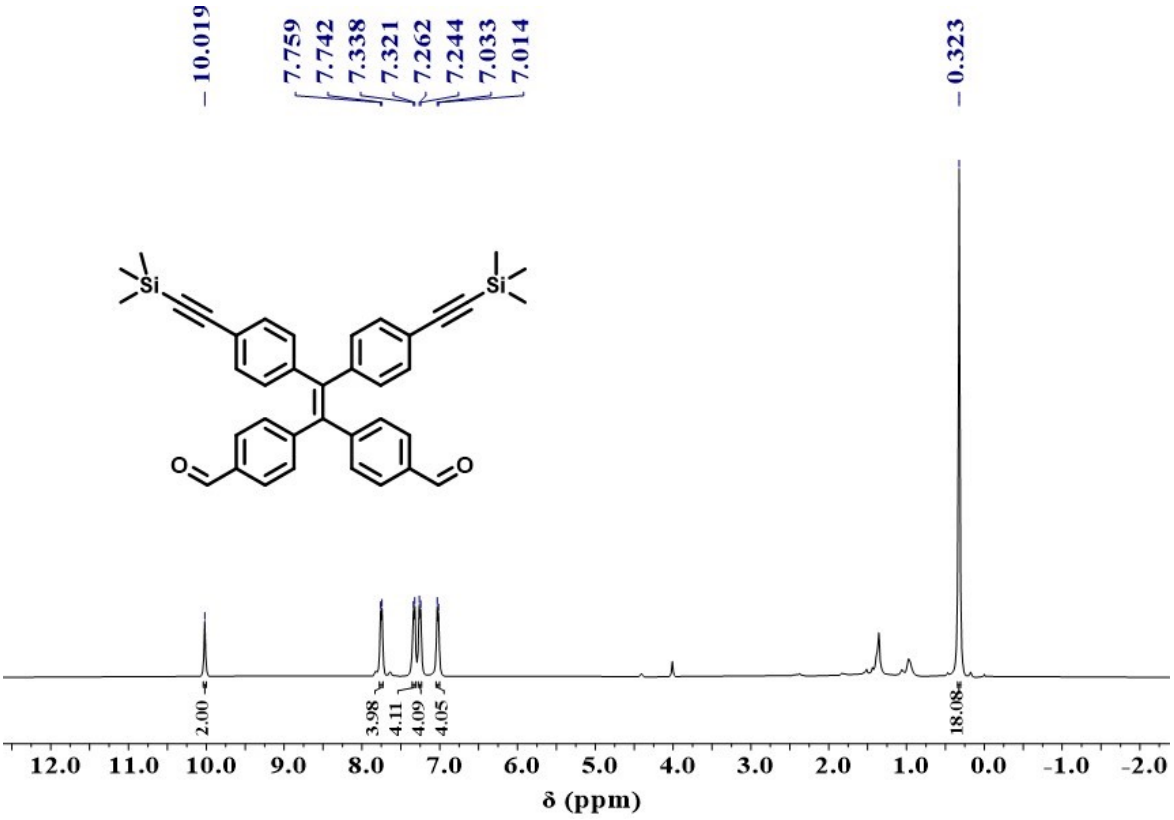

Fig. S1. ^{1}H NMR Spectrum of Compound **6**

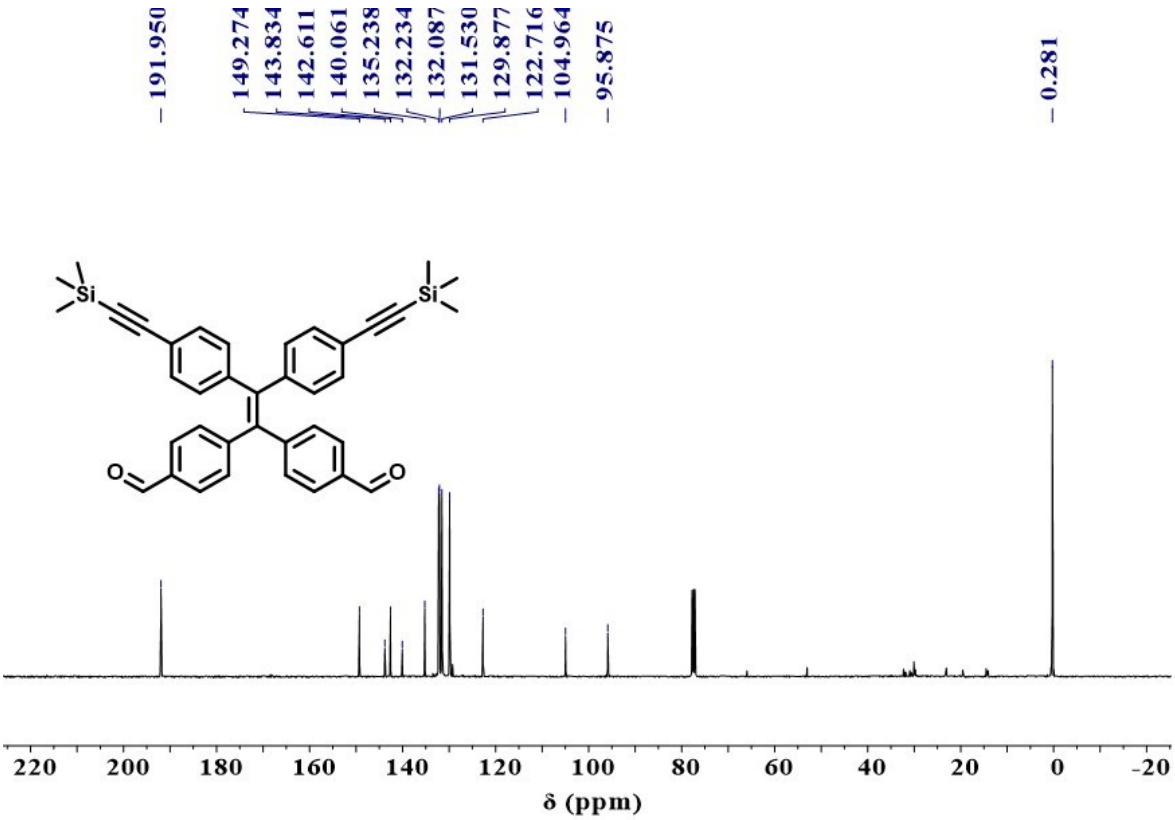

Fig. S2. ^{13}C NMR Spectrum of Compound **6**

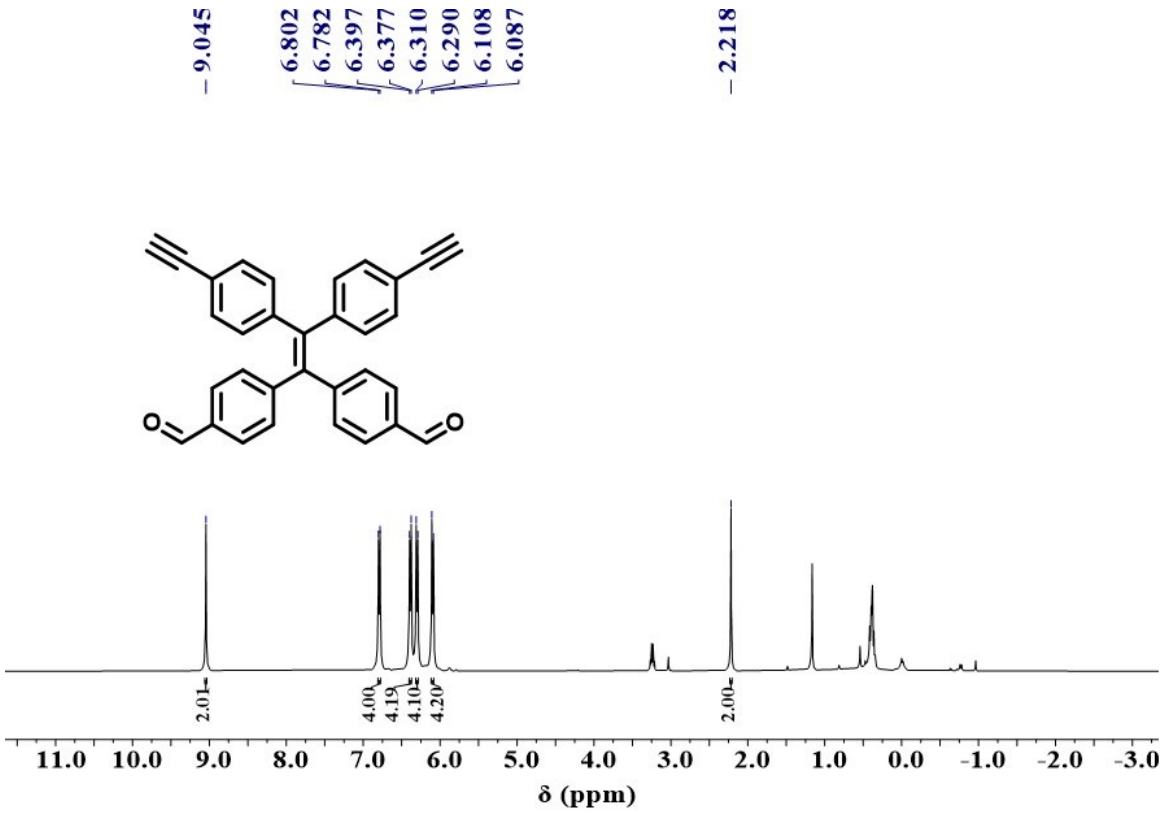

Fig. S3. ^{1}H NMR Spectrum of Compound **7**

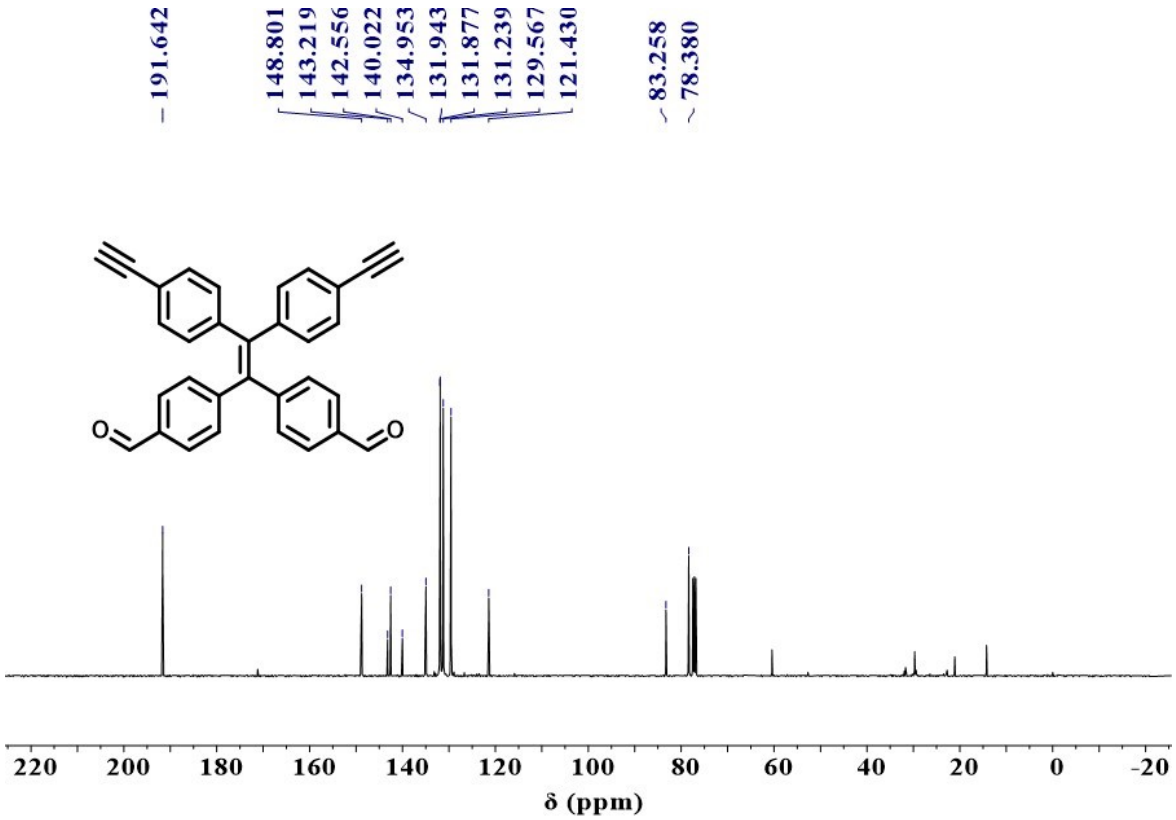

Fig. S4. ^{13}C NMR Spectrum of Compound **7**

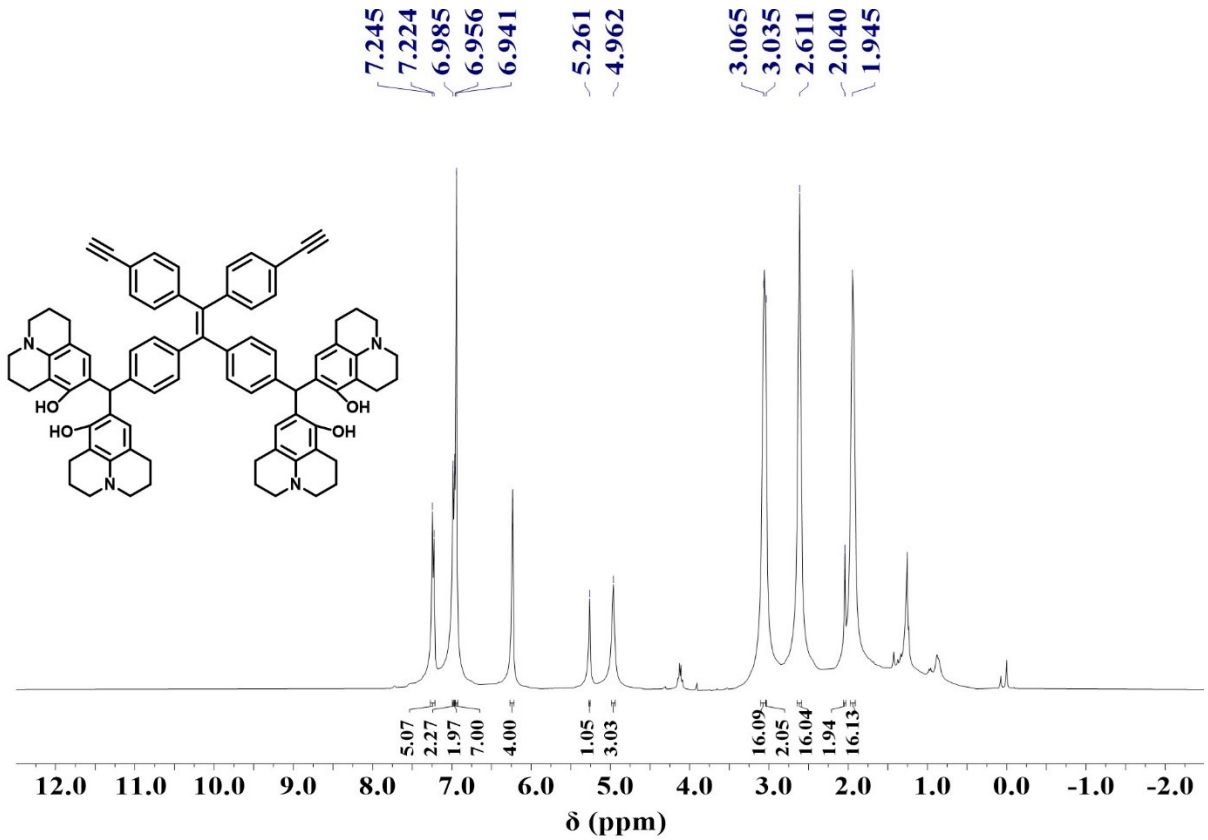

Fig. S5. ^{1}H NMR Spectrum of Compound **8**

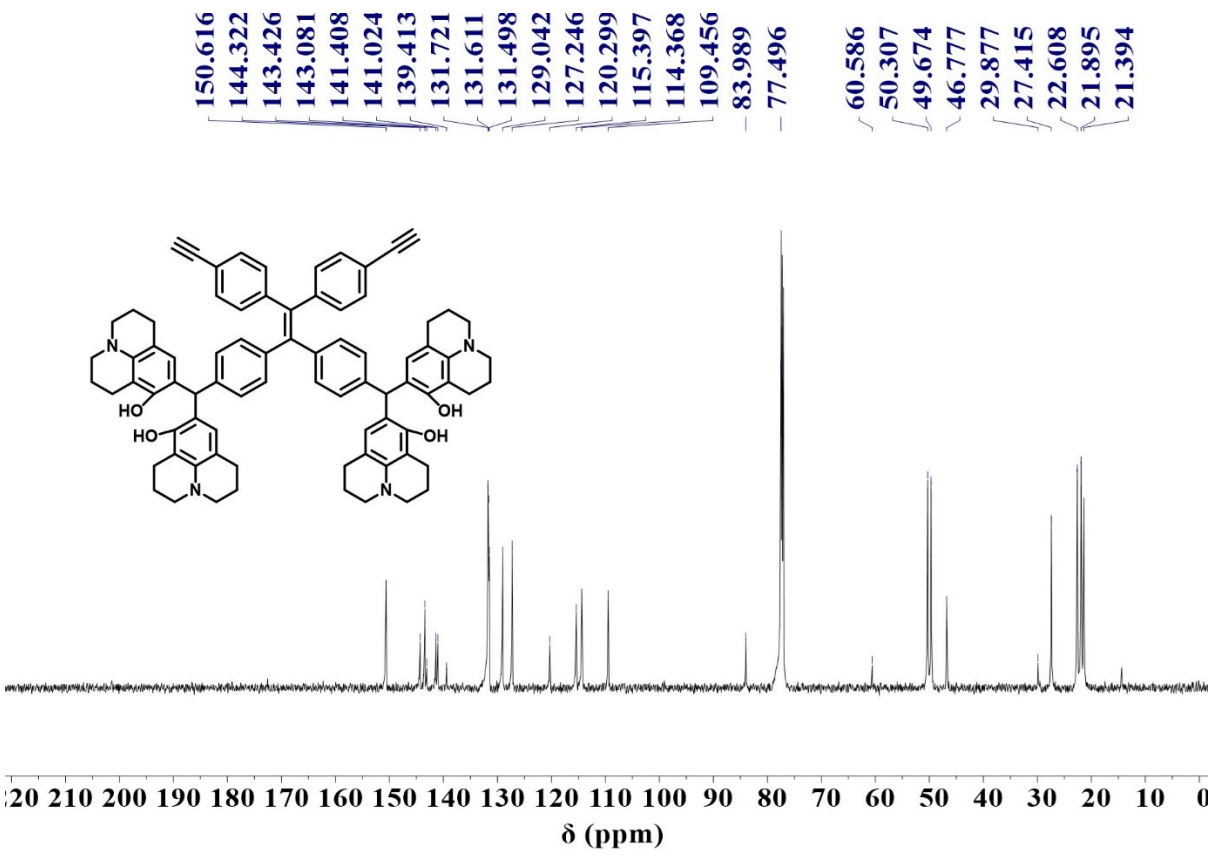

Fig. S6. ^{13}C NMR Spectrum of Compound **8**

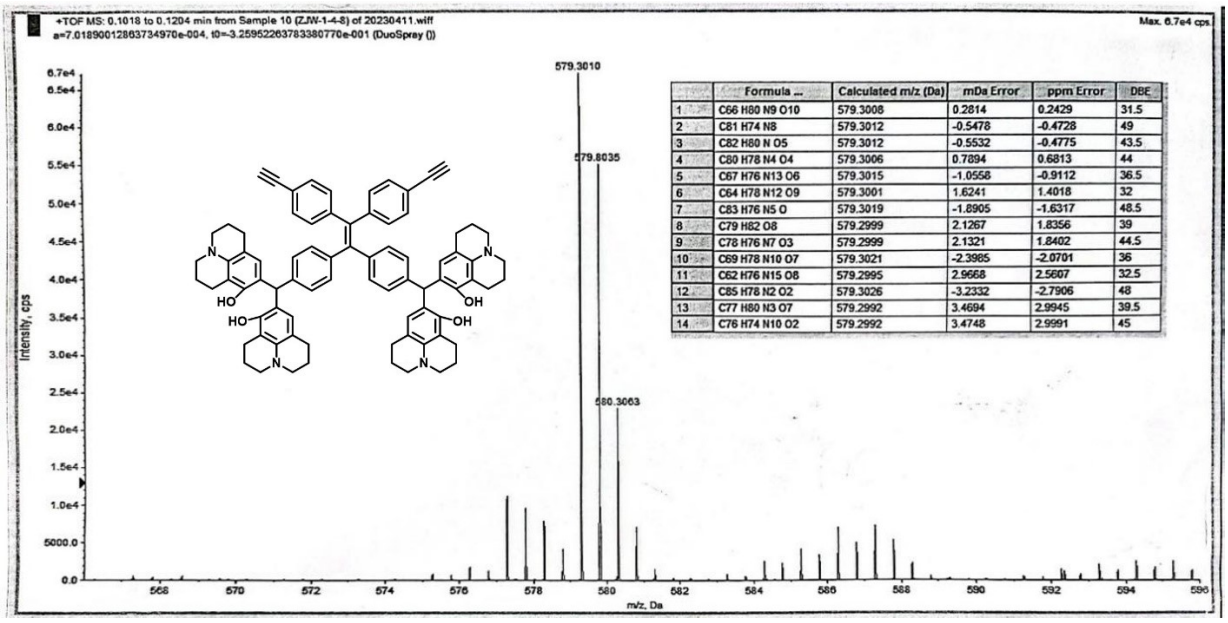

	Formula ...	Calculated m/z (Da)	mDa Error	ppm Error	DBE
1	C66 H80 N9 O10	579.3008	0.2814	0.2429	31.5
2	C81 H74 N8	579.3012	-0.5478	-0.4728	49
3	C82 H80 N O5	579.3012	-0.5532	-0.4775	43.5
4	C80 H78 N4 O4	579.3006	0.7894	0.6813	44
5	C67 H76 N13 O6	579.3015	-1.0558	-0.9112	36.5
6	C64 H78 N12 O9	579.3001	1.6241	1.4018	32
7	C83 H76 N5 O	579.3019	-1.8905	-1.6317	48.5
8	C79 H82 O8	579.2999	2.1267	1.8356	39
9	C78 H76 N7 O3	579.2999	2.1321	1.8402	44.5
10	C69 H78 N10 O7	579.3021	-2.3985	-2.0701	36
11	C62 H76 N15 O8	579.2995	2.9668	2.5607	32.5
12	C85 H78 N2 O2	579.3026	-3.2332	-2.7906	48
13	C77 H80 N3 O7	579.2992	3.4694	2.9945	39.5
14	C76 H74 N10 O2	579.2992	3.4748	2.9991	45

Fig. S7. MS Spectrum of Compound **8**

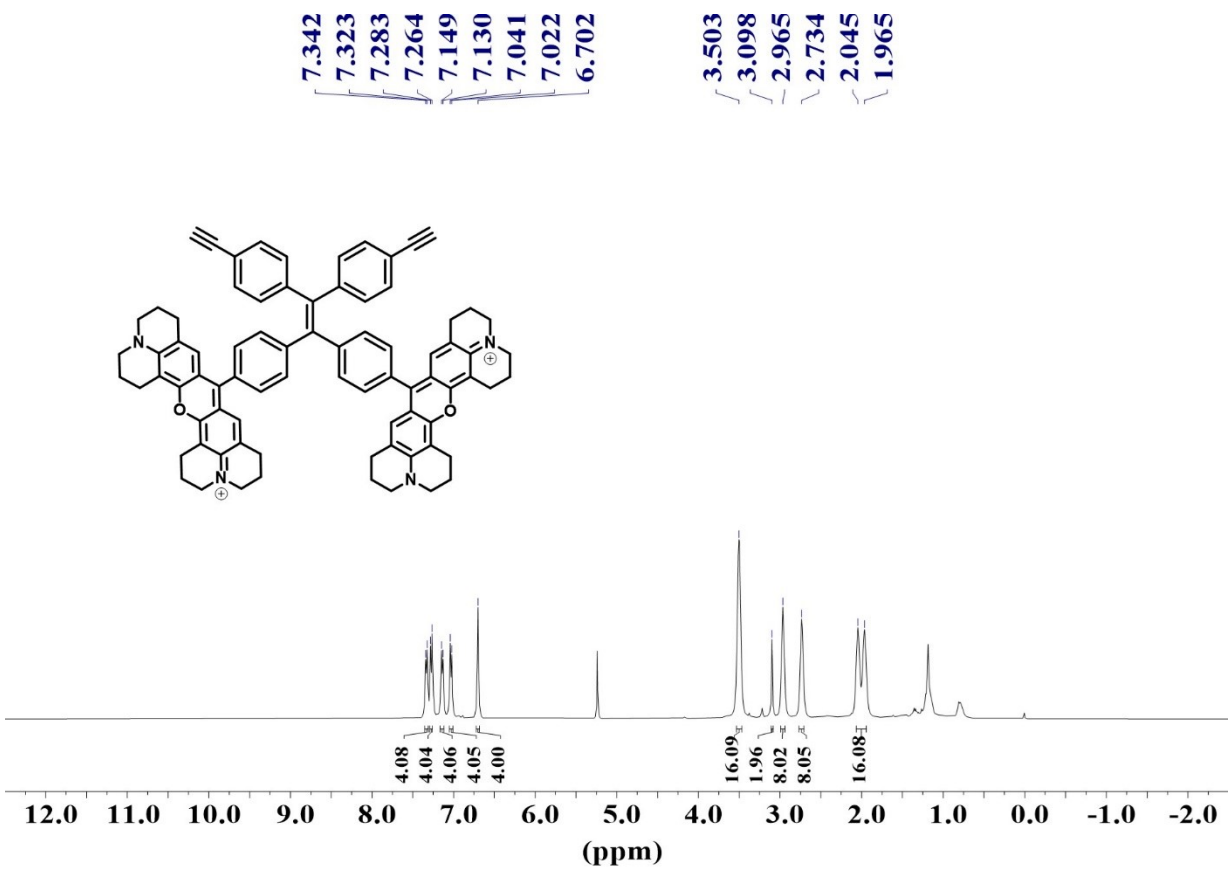

Fig. S8. ^{1}H NMR Spectrum of Compound **9**

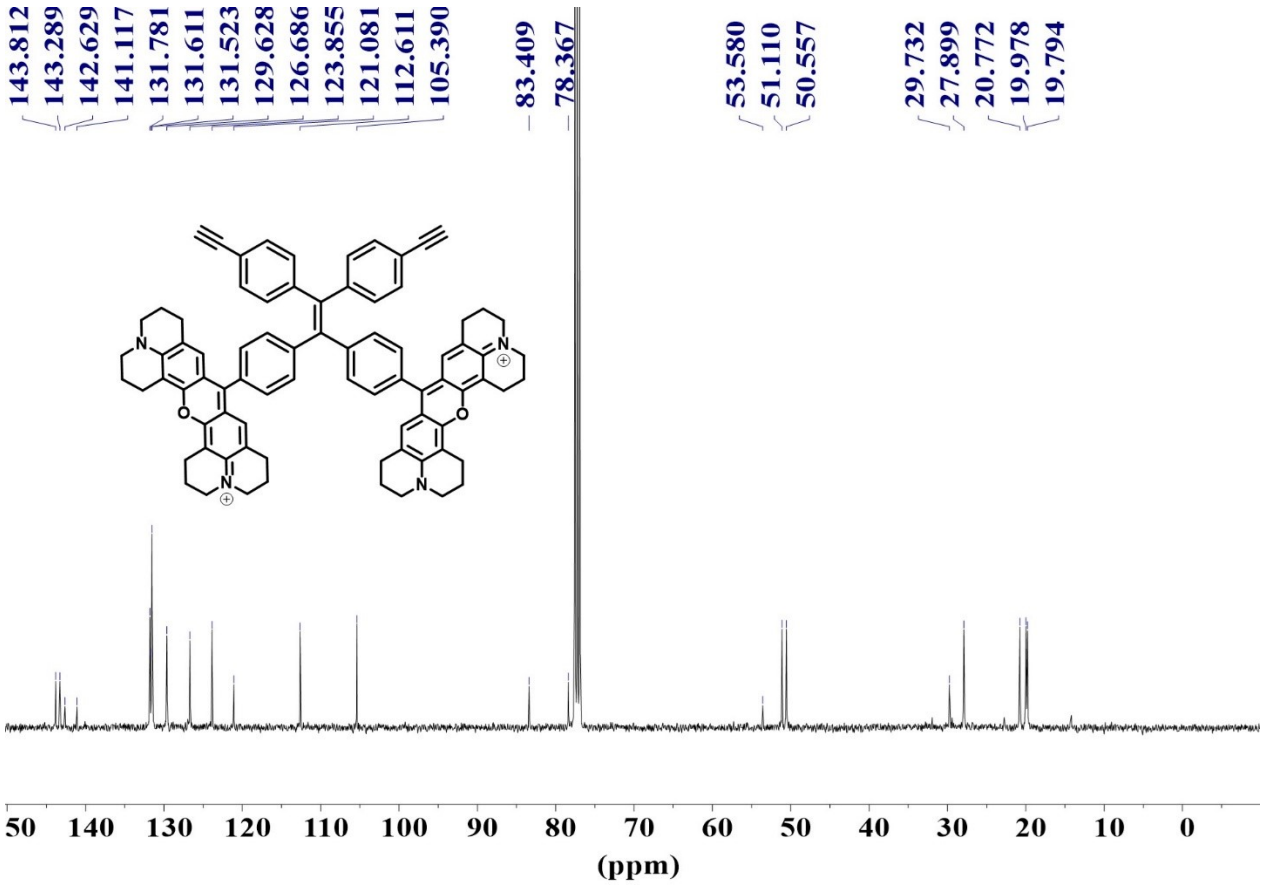

Fig. S9. ^{13}CNMR Spectrum of Compound **9**

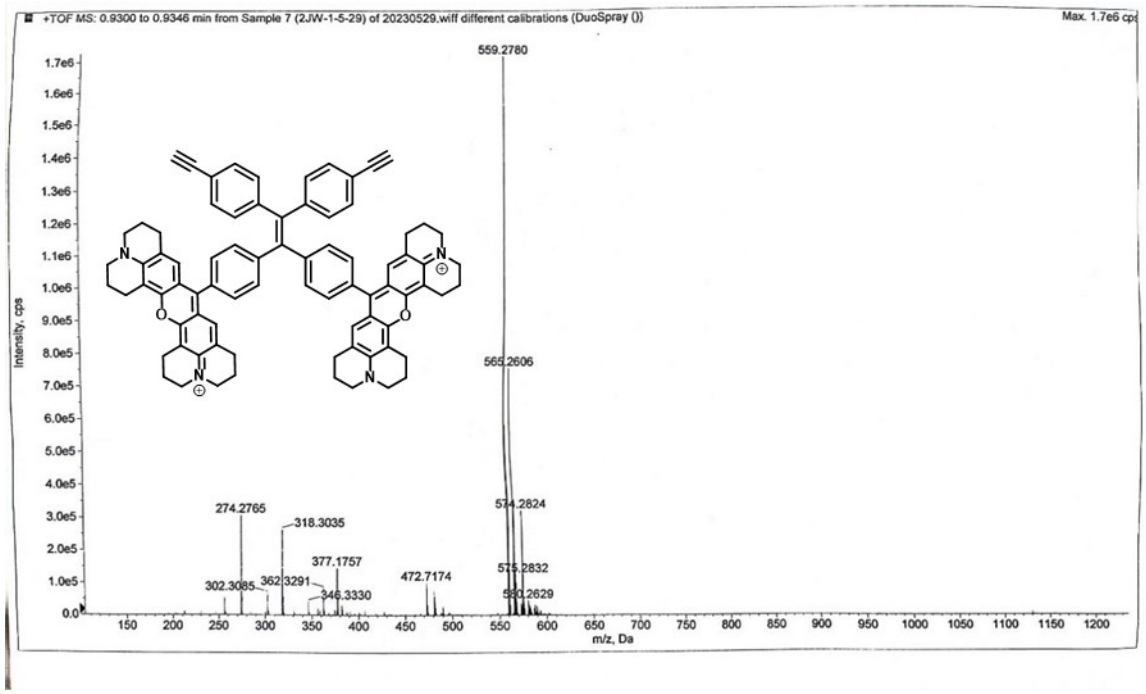

Fig. S10. MS Spectrum of Compound **9**

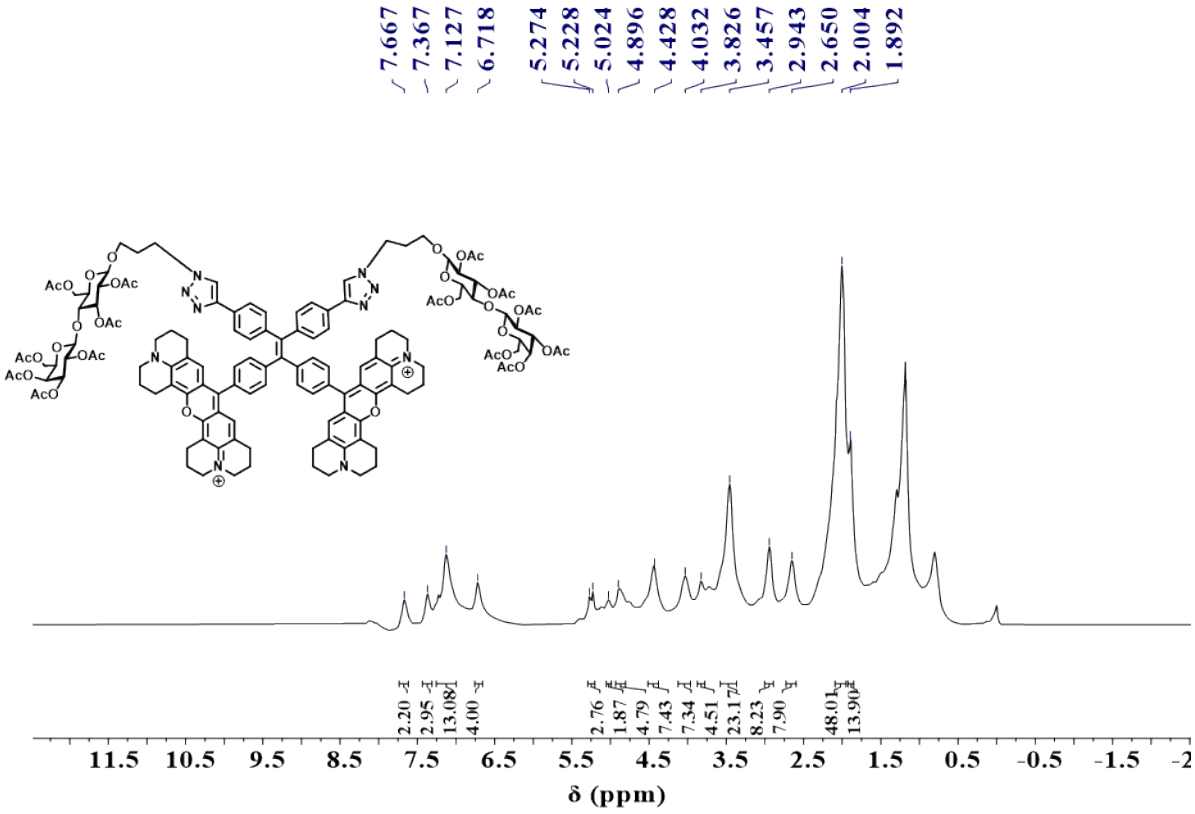

Fig. S11. ^{1}H NMR Spectrum of Compound **10**

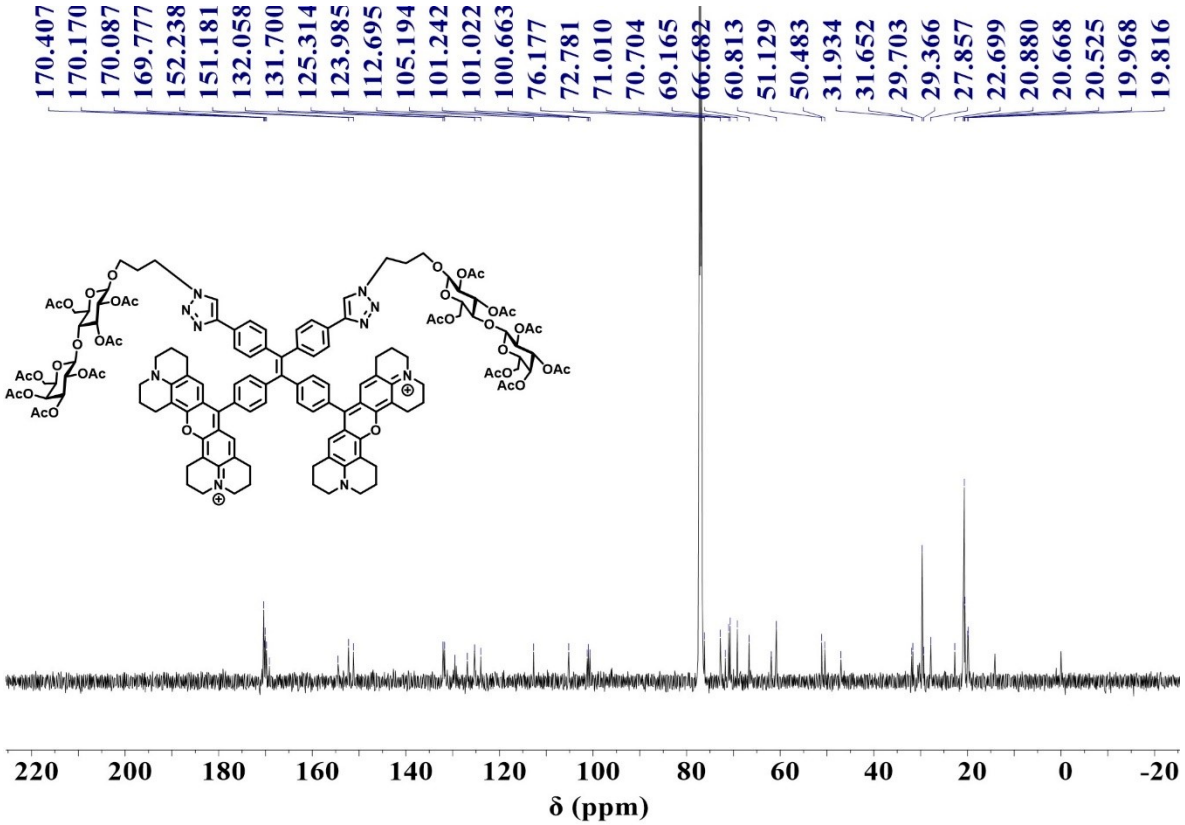

Fig. S12. ^{13}C NMR Spectrum of Compound **10**

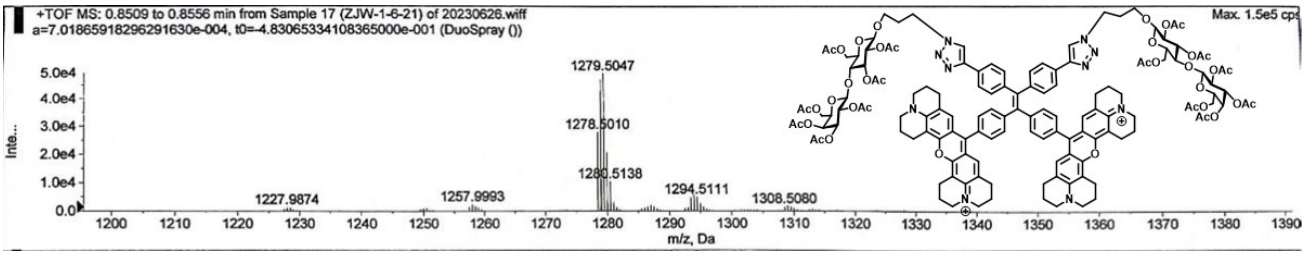

Fig. S13. MS Spectrum of Compound **10**

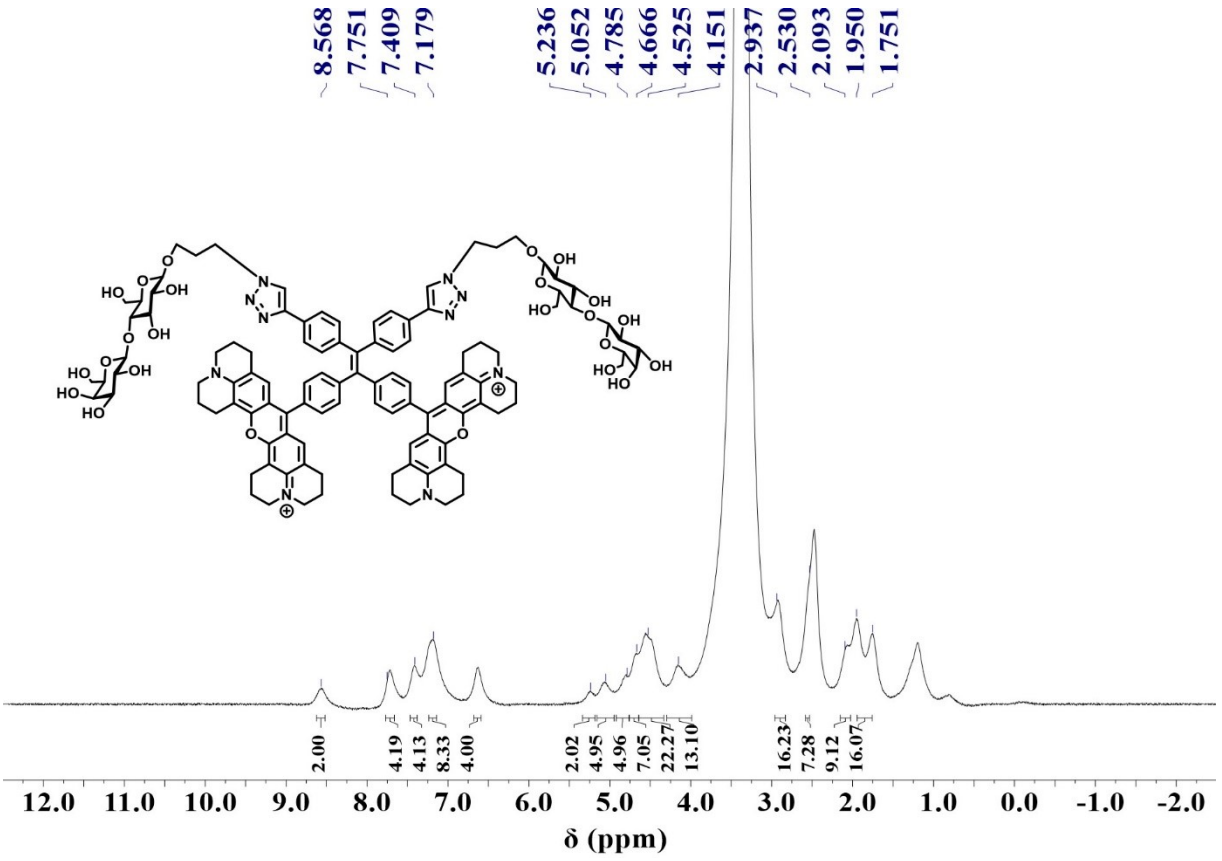

Fig. S14. ^{1}H NMR Spectrum of Compound **Lac-TR**

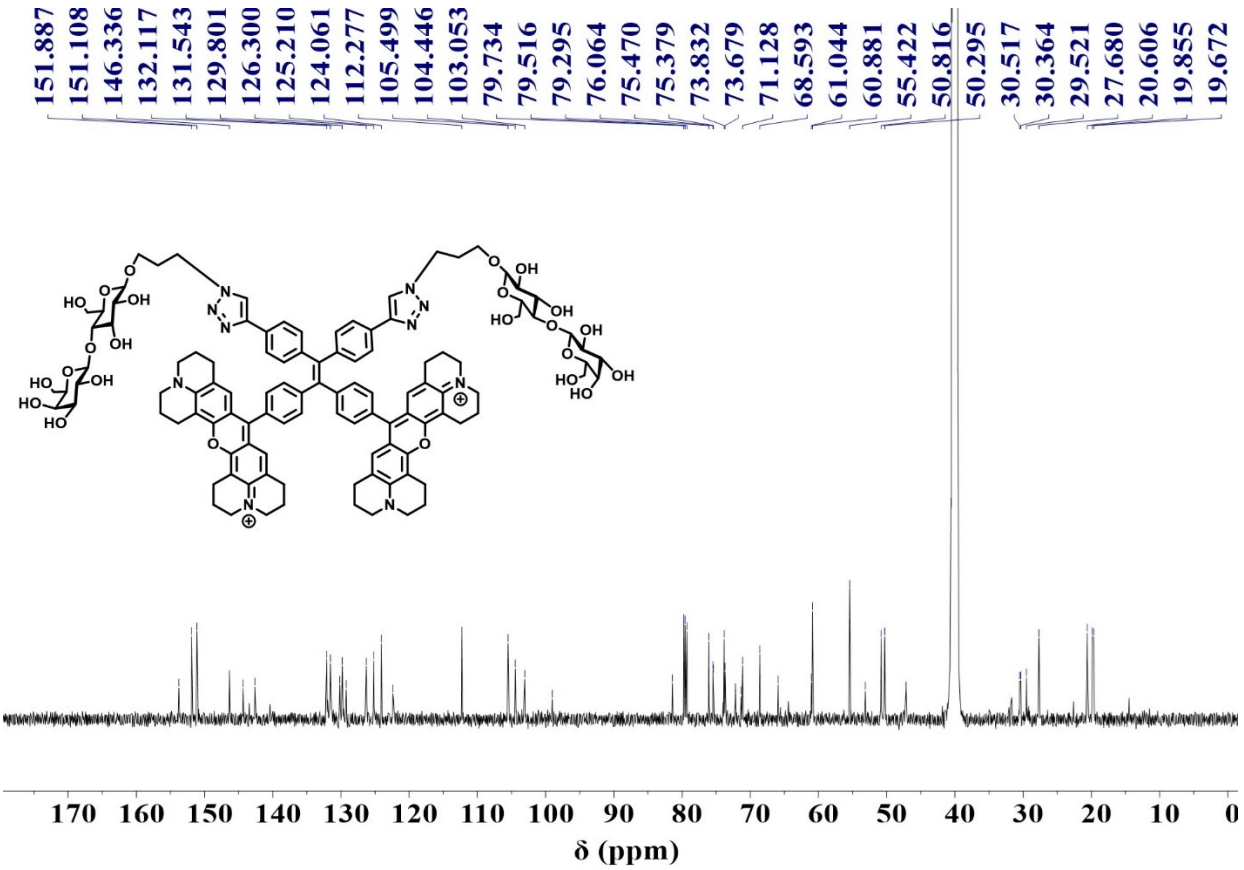

Fig. S15. ^{13}C NMR Spectrum of Compound **Lac-TR**

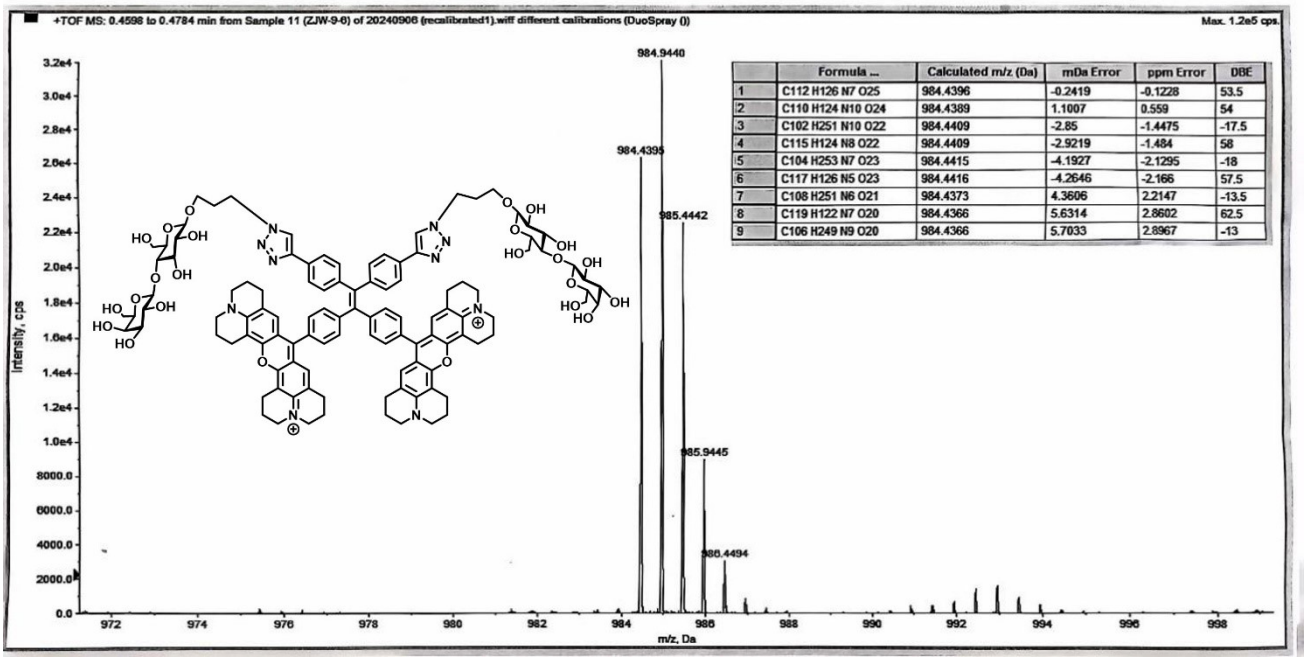

Fig. S16. MS Spectrum of Compound **Lac-TR**

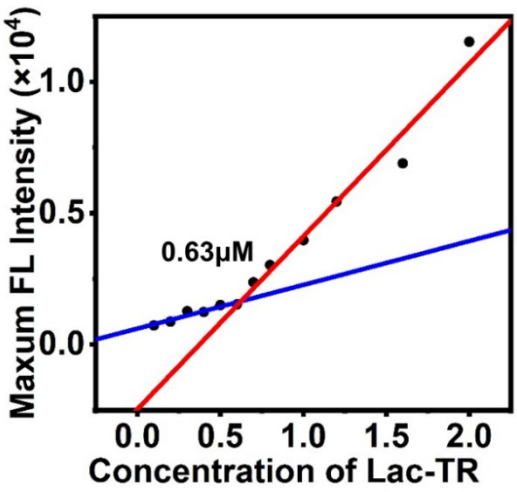

Fig. S17. The curve of fluorescence intensity at 650 nm versus the concentration of **Lac-TR** in PBS, pH = 7.4. The crosspoint corresponds to the CMC of **Lac-TRs**. λ_{ex} = 540 nm.

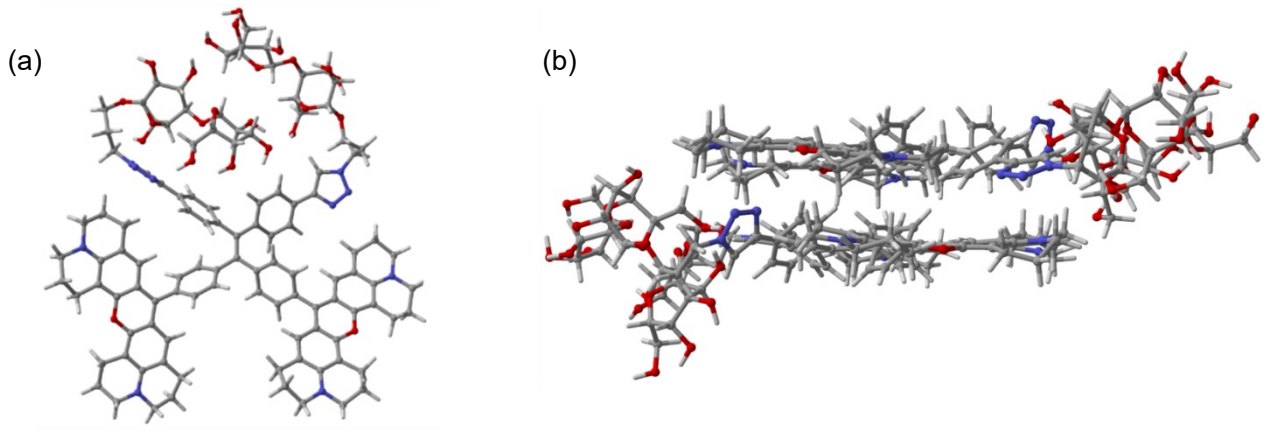

Fig. S18. The (a) Optimized **Lac-TR** monomer and (b) **Lac-TR** dimers structures.

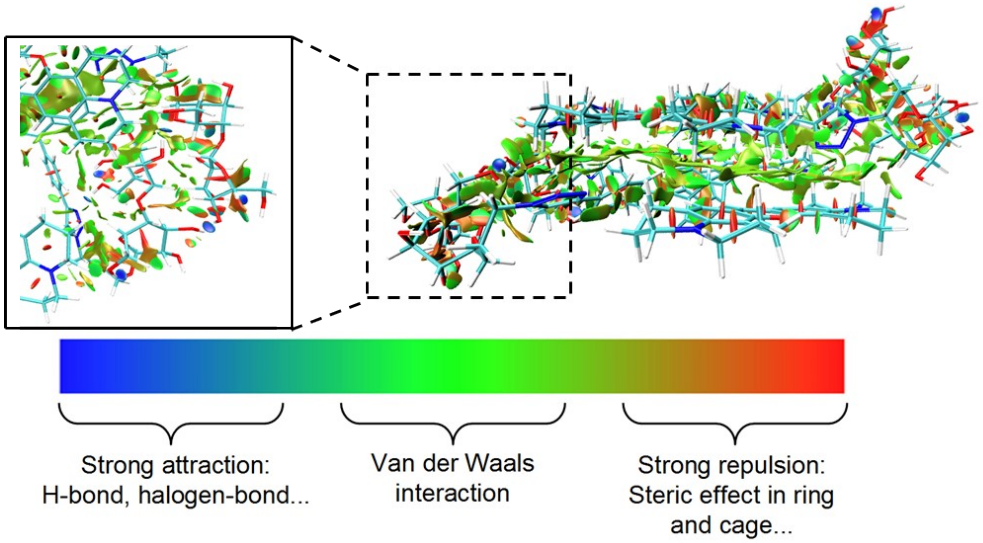

Fig. S19 Visual study of the isosurface of **Lac-TRs**, RDG = 0.5.

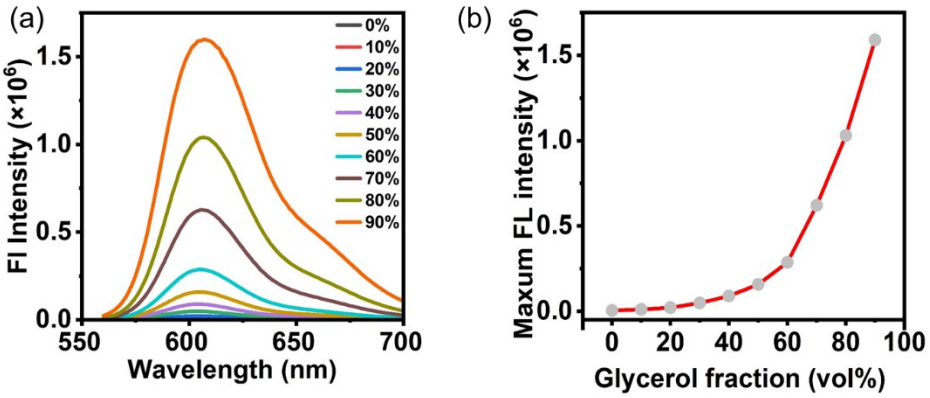

Fig. S20 Emission spectra of **Lac-TRs** (5μM) in PBS buffer mixtures with different glycerol fractions. (b) Maxum fluorescence emission intensity of **Lac-TRs** in PBS buffer mixtures with different glycerol fractions. λ_{ex} = 540 nm.

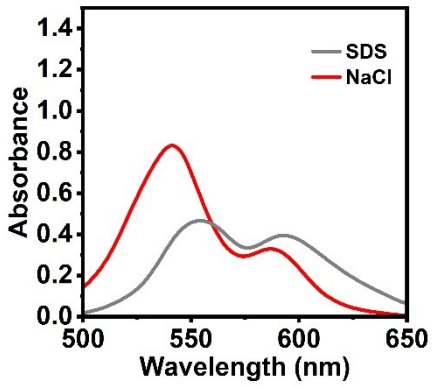

Fig. S21. UV−vis absorbance of **Lac-TRs** in NaCl (0.8 M) and SDS (0.2% w/v).

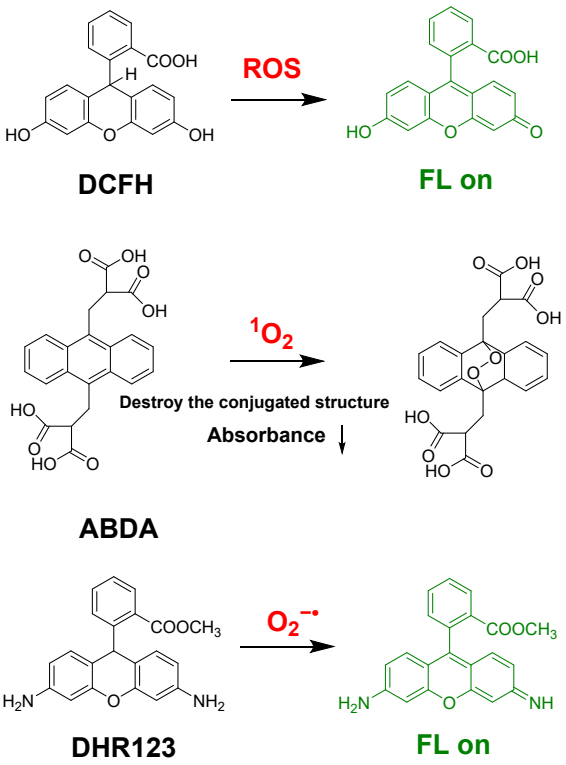

Fig. S22. Mechanism of detecting total reactive oxygen species by DCFH and singlet oxygen by ABDA and superoxide anion by DHR123.

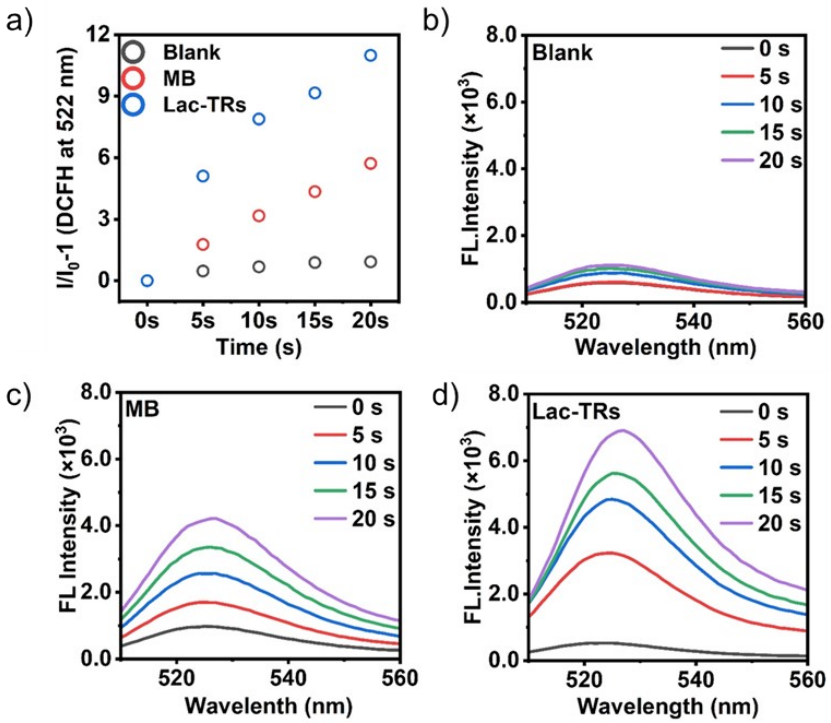

Fig. S23. (a) Plots of the fluorescence response of DCFH at 522 nm upon light irradiation (white light, 40 mW/cm^2) for different time intervals in the presence of **Lac-TRs**, MB, or DCFH. Fluorescence emission spectra of DCFH in the presence of photosensitizers under the white light irradiation with different time in PBS. (b) just DCFH, (c) MB, (d) Lac-TRs white light irradiation (white light, 40 mW/cm^2), λ_{ex} = 488 nm.

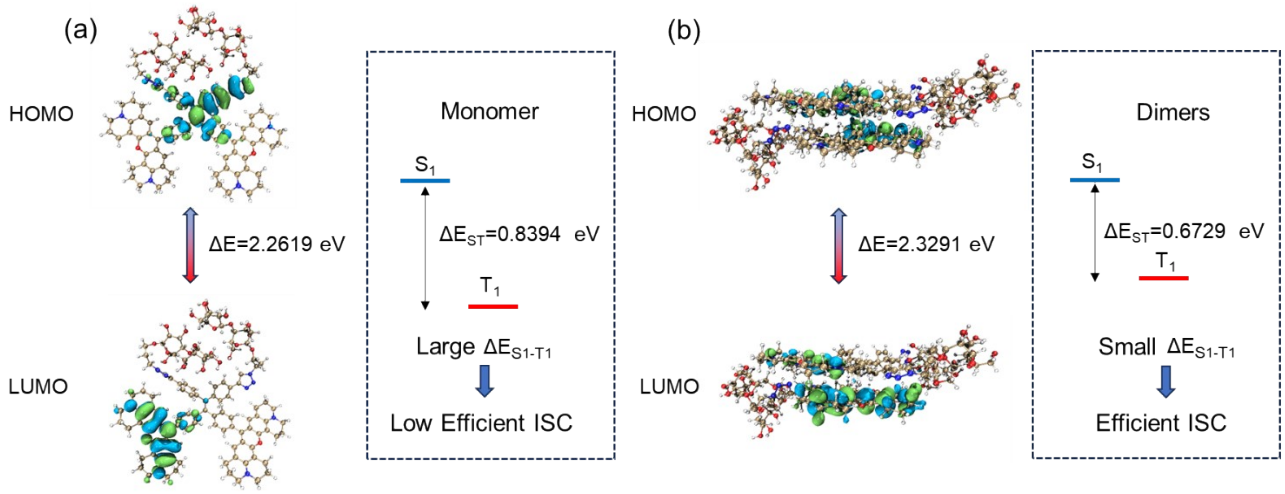

Fig. S24. Calculated HOMO-LUMO geometries and S_1,T_1 energy levels for the optimized structure of (a) **Lac-TR** and (b) **Lac-TRs**

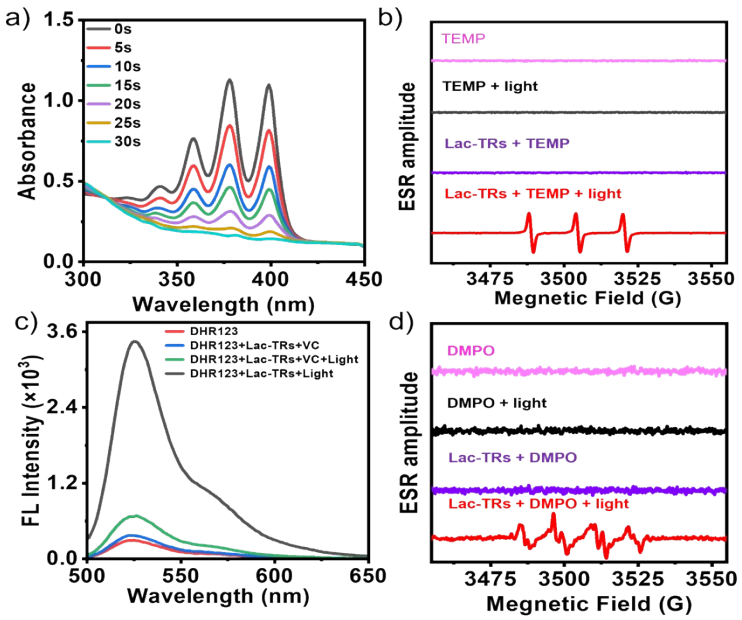

Fig. S25. (a) UV-Vis spectra of ABDA in PBS under white light irradiation (40 mW/cm^2) in the presence of **Lac-TRs** (10 μM). (b) ESR signals of $^1O_2$ with **Lac-TRs** under light irradiation. (c) Fluorescence emission spectra of DHR123 in the presence of **Lac-TRs** under the white light irradiation with or without Vc. (d) ESR signals of $O_2^{-\bullet}$ with Lac-TRs under light irradiation.

The potential formation mechanism of superoxygen was further investigated through electrochemical methods. In the photodynamic process, superoxide anion can be generated through the following reaction: $PS^{\bullet-} + {}^3O_2 \rightarrow PS + O_2^{\bullet-}$. The prerequisite for this reaction is the formation of $PS^{\bullet-}$. Prior to this reaction, the formation of $PS^{\bullet-}$ can occur through the following reaction: $PS(T_1) + PS(S_0) \rightarrow PS^{\bullet+} + PS^{\bullet-}$. The Gibbs free energy of single electron transfer for the Lac-TR molecules were calculated with Rehm-Weller equation (as follow).

$$\Delta G = e\left[E_{D^{+\bullet}/D} - E_{A/A^{-\bullet}} - E_{00}\right] - \frac{e^2}{4\pi\varepsilon_s\varepsilon_0 R_{cc}} - \frac{e^2}{8\pi\varepsilon_0}\left(\frac{1}{r^+} + \frac{1}{r^-}\right)\left(\frac{1}{\varepsilon_{ref}} - \frac{1}{\varepsilon_s}\right)$$

$$\approx e\left[E_{D^{+\bullet}/D} - E_{A/A^{-\bullet}} - E_{00}\right]$$

For the **Lac-TR** molecule, the Gibbs free energy of electron transfer was calculated based on the equation $\Delta G \approx e\,[E_{ox}-E_{red}-E_{00}]$, where E_{ox} is onset potential for one electron oxidation; E_{red} is the onset potential for one electron reduction; The excited state energy E_{00} can be estimated at the intersection point of the normalized absorbance and emission spectrum of **Lac-TR**[9,10], calculated as 2.053 eV. The obtained ΔG is less than 0, indicating that the charge transfer from the excited state **Lac-TR** to the ground state **Lac-TR** is thermodynamically feasible.

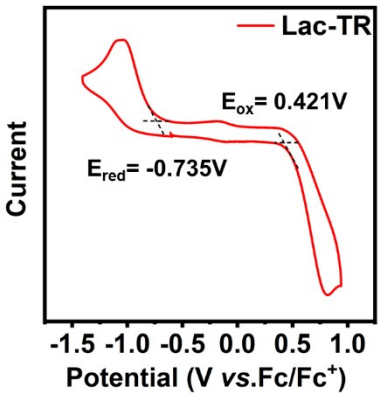

Fig. S26a. Cyclic voltammogram of **Lac-TR** with 0.1 M $(n\text{-}Bu)_4N^+PF_6^-$ as a supporting electrolyte, Ag/Ag+ as a reference electrode, platinum- carbon composite as a working electrode and Pt wire as a auxiliary electrode; scan rate, 100 mV/s; Fc/Fc+ was used as an external reference.

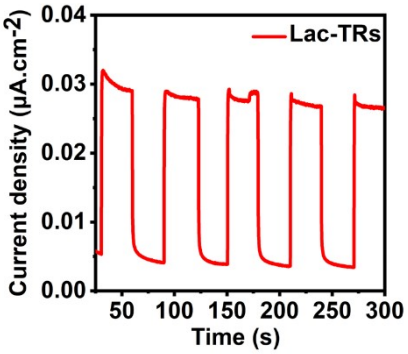

Fig. S26b. Representative photocurrent responses of **Lac-TRs** under light illumination.

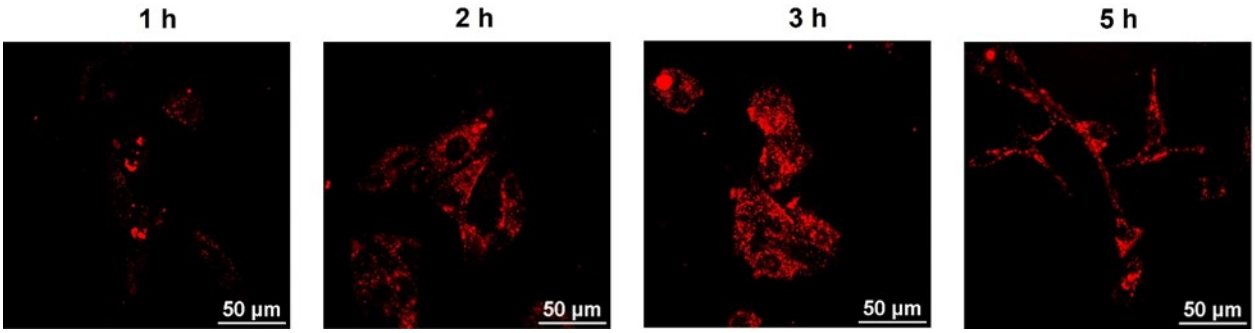

Fig. S27. Confocal fluorescence images of HepG2 cells incubated with 10 μM **Lac-TRs** for different time. λ_{ex} = 561nm, λ_{em} = 580-700 nm. Scale bar: 50 μm.

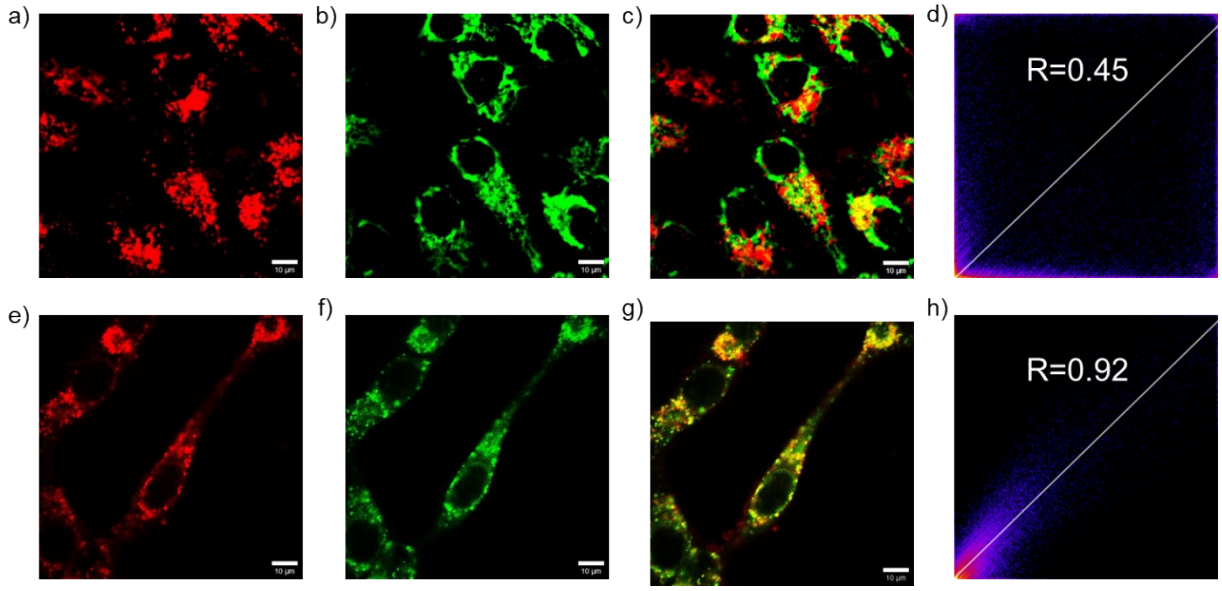

Fig. S28. Subcellular colocalization fluorescence imaging in HepG2 cells. Confocal fluorescence image of live HepG2 cells stained with **Lac-TRs** (10 μM) and commercial dyes. (a) and (e) **Lac-TRs** channel (red); (b) Mito Tracker channel (green); (c) merged images of (a) and (b); (f) Lyso Tracker channel (green); (g) merged images of (e) and (f); (d) and (h): Scatter plot of co-localization Pearson coefficient. Scale bar: 10 μm

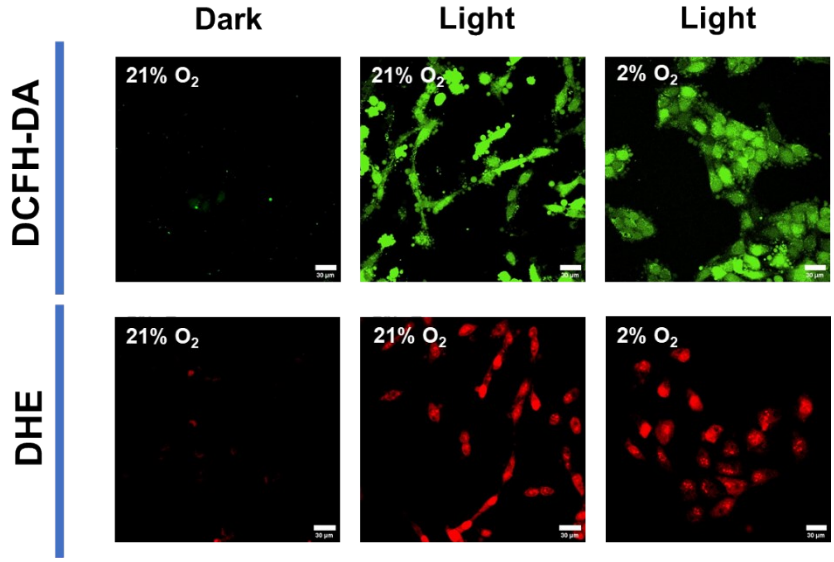

Fig. S29. ROS detection in HepG2 cells under normoxia (21% O_2) and hypoxia (2% O_2) conditions using DCFH-DA (λ_{ex} = 488 nm, λ_{em} = 500-550 nm, scale bar = 30 μm), DHE (λ_{ex} = 488 nm, λ_{em} = 580-620 nm, scale bar = 30 μm) as the ROS, $O_2^{-\bullet}$ fluorescence indicator, respectively. Scale bar: 30 μm.

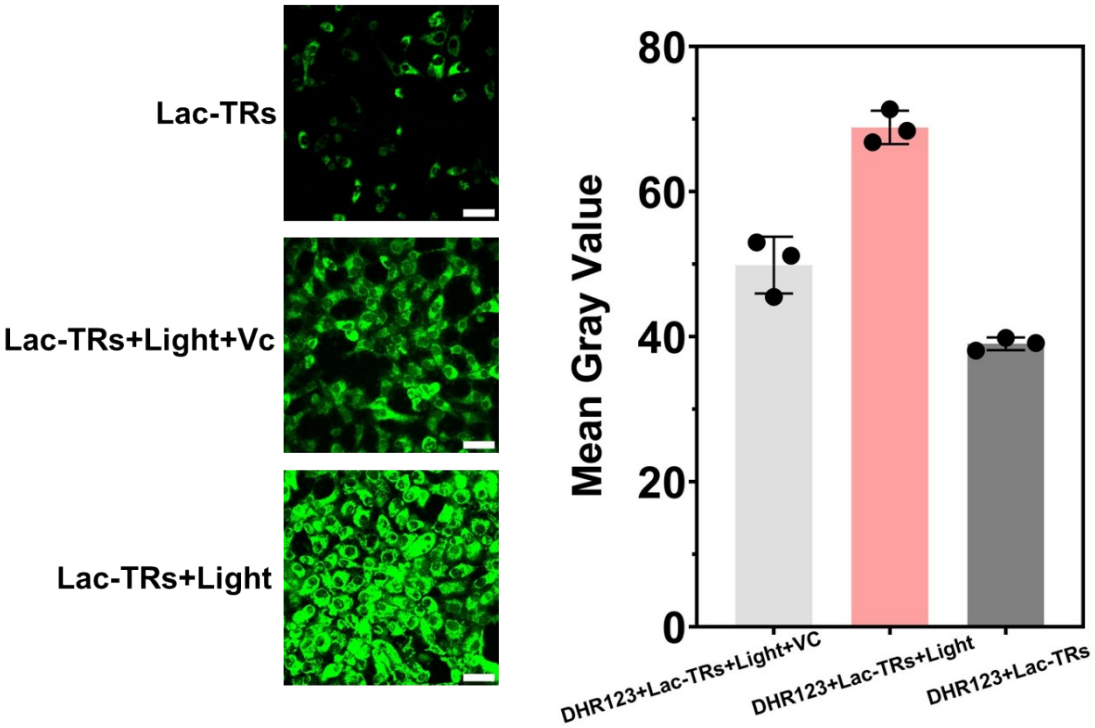

Fig. S30. Intracellular Type I ROS detection inside **Lac-TRs**+Dark, **Lac-TRs**+Light and **Lac-TRs** +Light+Vc treated HepG2 cells, accessed by DHR123. λ_{ex} = 488 nm, λ_{em} = 500-550 nm, scale bar = 50 μm

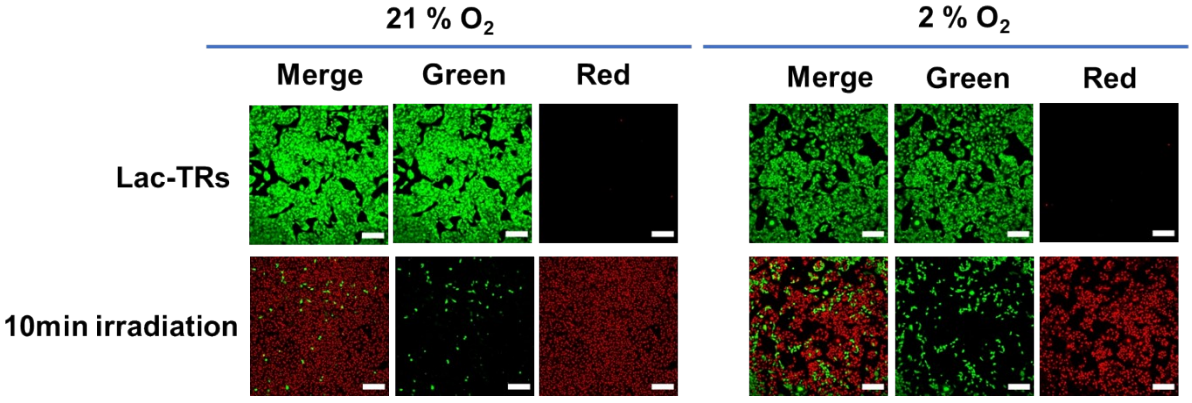

Fig. S31. With white light (40 mW/cm^2) irradiation or not cytotoxicity observed for HepG2 cells incubated with **Lac-TRs** (10μM) under hypoxia and normoxia. Live/Dead cells are detected as green or red by staining with Calcein-AM and PI. Scale bar = 200 μm

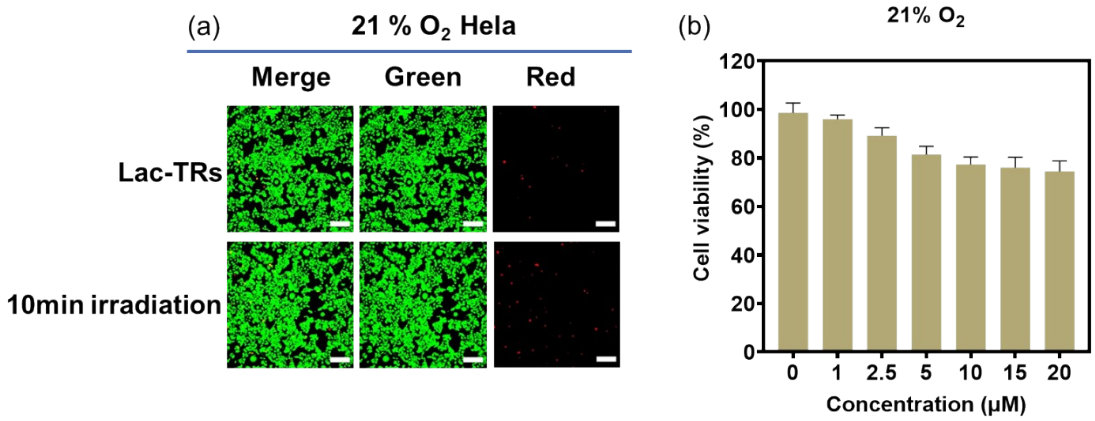

Fig. S32. (a) With white light (40 mW/cm^2) irradiation or not cytotoxicity observed for Hela cells incubated with **Lac-TRs** (10μM) under normoxia. Live/Dead cells are detected as green or red by staining with Calcein-AM and PI. scale bar = 200 μm. (b) Cell viability of Hela cells after being incubated with different concentrations of **Lac-TRs** with white light irradiation of (40 mW/cm^2) under normoxia.

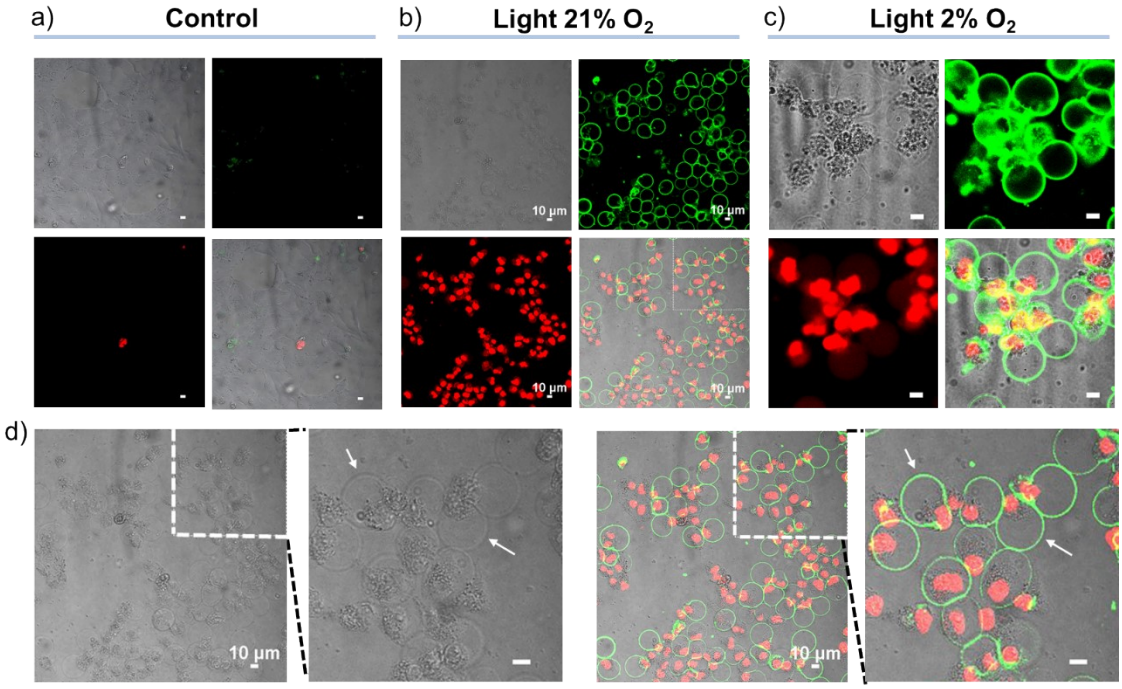

Fig. S33. Annexin V-FITC/PI co-staining assay, red fluorescence of PI (λex = 488 nm, λem =580–620 nm) and green fluorescence of Annexin V (λ_{ex} = 488 nm, λ_{em} = 500–550 nm). (a) **Lac-TRs** alone and (b) **Lac-TRs** +light under normoxia. (c) **Lac-TRs** + light under hypoxia. Scale bars: 10 μm.(d) Enlarged view of the bright field and merged field of (b).

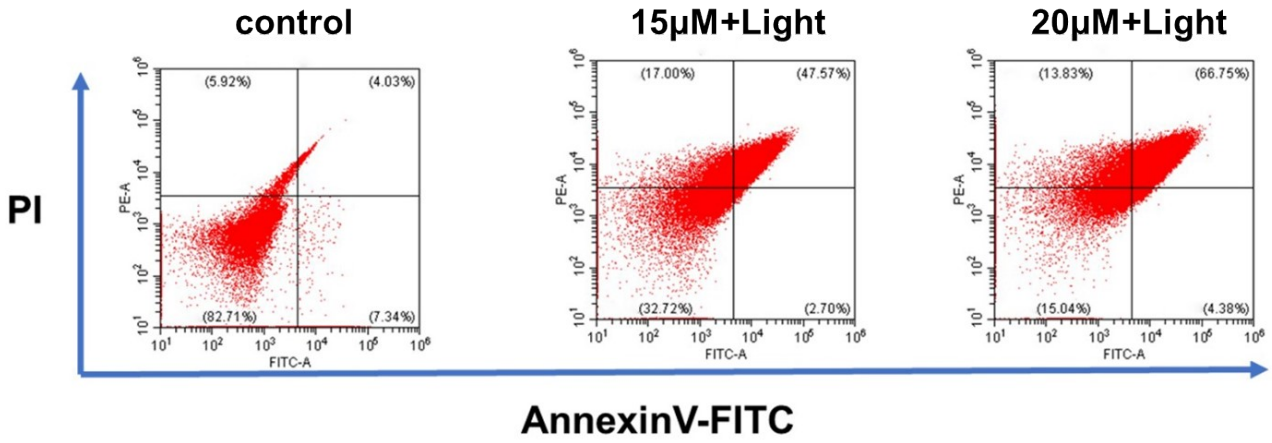

Fig. S34. Flow cytometry assays on HepG2 cells treated with 15 μM or 20 μM **Lac-TRs** under light irradiation (400-800 nm,40 mW/cm^2).

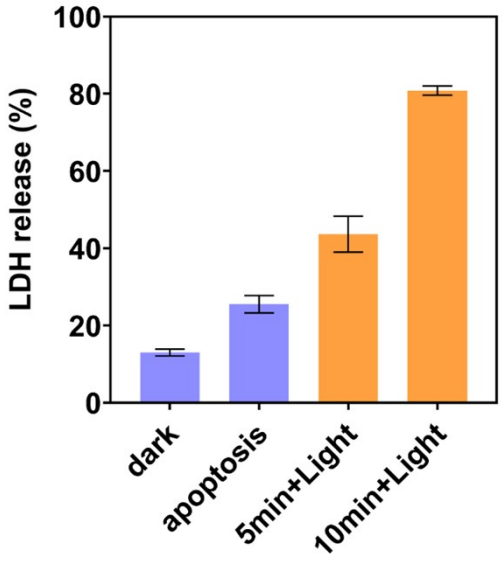

Fig. S35 Quantification of LDH release. Lactate dehydrogenase (LDH) release from HepG2 cells treated with **Lac-TRs** (10 μM) by no light irradiation , apoptosis induced by starvation and 5 min or 10 min of 40 mW/cm^2 light irradiation.

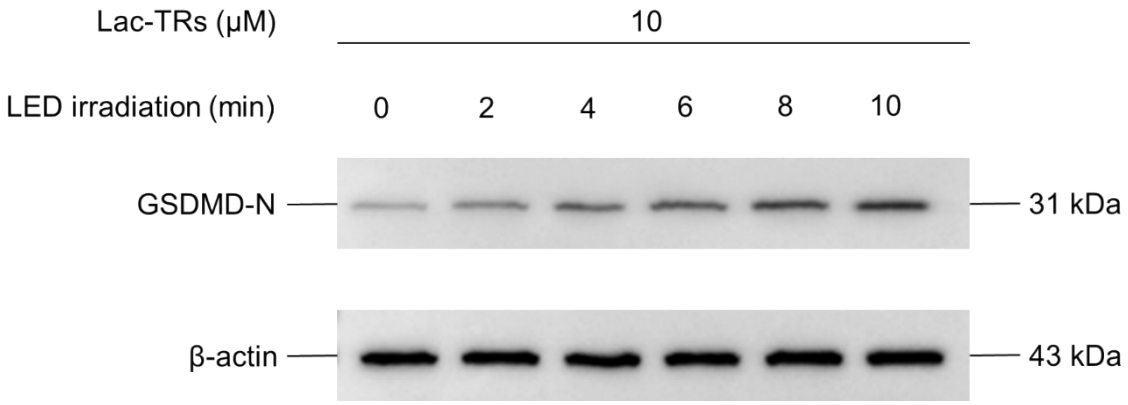

Fig. S36. Western blot of GSDMD-N fragment in **Lac-TRs** treated cells under different light irradiation times.

References:

1. M. J. Frisch, G. W. Trucks, H. B. Schlegel, G. E. Scuseria, M. A. Robb, J. R. Cheeseman, G. Scalmani, V. Barone, B. Mennucci, G. A. Petersson, H. Nakatsuji, M. Caricato, X. Li, H. P. Hratchian, A. F. Izmaylov, J. Bloino, G. Zheng, J. L. Sonnenberg, M. Hada, M. Ehara, K. Toyota, R. Fukuda, J. Hasegawa, M. Ishida, T. Nakajima, Y. Honda, O. Kitao, H. Nakai, T. Vreven, J. A. Montgomery, Jr., J. E. Peralta, F. Ogliaro, M. Bearpark, J. J. Heyd, E. Brothers, K. N. Kudin, V. N. Staroverov, T. Keith, R. Kobayashi, J. Normand, K. Raghavachari, A. Rendell, J. C. Burant, S. S. Iyengar, J. Tomasi, M. Cossi, N. Rega, J. M. Millam, M. Klene, J. E. Knox, J. B. Cross, V. Bakken, C. Adamo, J. Jaramillo, R. Gomperts, R. E. Stratmann, O. Yazyev, A. J. Austin, R. Cammi, C. Pomelli, J. W. Ochterski, R. L. Martin, K. Morokuma, V. G. Zakrzewski, G. A. Voth, P. Salvador, J. J. Dannenberg, S. Dapprich, A. D. Daniels, O. Farkas, J. B. Foresman, J. V. Ortiz, J. Cioslowski, and D. J. Fox, Gaussian, Inc., Wallingford CT, **2013**.

2. J. Tirado-Rives and W. L. Jorgensen, *J. Chem. Theory. Comput.*, 2008, **4**, 297-306.

3. S. Grimme, J. Antony, S. Ehrlich and H. Krieg, *J. Chem. Phys.*, 2010, **132**, 154104.

4. S. Grimme, S. Ehrlich and L. Goerigk, *J. Comput. Chem.*, 2011, **32**, 1456-1465.

5. T. Lu and F. Chen, *J. Comput. Chem.*, 2012, **33**, 580-592.

6. M. Hou, Y. C. Liu, W. Zhou, J. D. Zhang, F. D. Yu, Y. Zhang, G. J. Liu and G. W. Xing, *Chemistry- An Asian journal*, 2021, **16**, 2014-2017.

7. H. W. Hsieh, R. A. Davis, J. A. Hoch and J. Gervay-Hague, *Chemistry*, 2014, **20**, 6444-6454.

8. Y. C. Liu, W. Du, G. J. Liu, W. Zhou, X. J. Gao and G. W. Xing, *Chemistry- An Asian journal*, 2021, **16**, 277-281.

9. D. Rehm and A. Weller, *Isr. J. Chem.*, 1970, **8**, 259-271.

10. K. Teng, L. Niu and Q. Yang, *J. Am. Chem. Soc.*, 2023, 145, 4081-4087.